A Thesis

on

Simultaneous Determination of Refractive Index and Thickness of Very Thin Films by Ellipsometry

by

Raghuvir Rai

Grant Number: NASA Grant NGR-39-009-042

National Aeronautics and Space Administration
Goddard Space Flight Center
Greenbelt, Maryland

Project Supervisor: K. Vedam

The Pennsylvania State University

The Graduate School

Department of Materials Science

Simultaneous Determination of Refractive Index and Thickness of Very Thin Films by Ellipsometry

A thesis in

Solid State Science

by

Raghuvir Rai

Submitted in partial fulfillment
of the requirements
for the degree of

Master of Science

December 1967

Approved:

_____

_____
Associate Professor of Solid State Science, Thesis Advisor

_____

_____
Chairman, Solid State Science Section

ACKNOWLEDGMENTS

The author wishes to express his sincere thanks and deep sense of appreciation to Dr. K. Vedam for suggesting the problem, and for his kind guidance and constructive criticism during all phases of the investigation.

Thanks are also due to Dr. F. Lukes and Dr. R. Srinivasan for their assistance in calibration of the ellipsometer and the theoretical aspects of the problem, respectively.

The help of Mr. John Labenski in building the instrumentation and of Mr. Ed Jones for sample preparation is gratefully acknowledged.

The financial support of NASA, under the grant NGR-39-009-042, is gratefully acknowledged.

TABLE OF CONTENTS

LIST OF TABLES

LIST OF FIGURES

I. INTRODUCTION

Ellipsometric studies are concerned with the change in the state of polarization of reflected light from a "clean" surface or from a substrate with a film on it. When a clean surface without any contamination is used as the reflecting surface, it is possible to measure its optical constants from these studies. Conversely, if the optical constants of the substrate are known it is possible to determine the thickness and refractive index of any film on it. The values of the refractive index and the thickness of the film can be accurate as the procedure involves only an analysis of the polarized light, and no photometry is involved in the measurements.

Historical Background

The foundation on which ellipsometry is based are the Fresnel formulae which are the basic and fundamental work of Augustin Fresnel early in the nineteenth century. These formulae indicate that when light is reflected, e.g., at the air-water surface, the two components vibrating in and perpendicular to the plane of incidence after reflection, undergo a phase shift of 180° or 0°, and furthermore the parallel component becomes zero at a certain angle called the Brewster angle.

Drude was the first to test the validity of Fresnel formulae. Ellipsometry is based on the fundamental work of Drude[1] on the optical properties of light reflected from absorbing solids--like metals with and without a film on their surfaces. Drude derived a theoretical expression for the optical thickness of a film and the optical constants of the substrate upon which the film was deposited, in terms of two parameters characterizing the ellipse representing the reflected light. These two parameters were: (i) the ratio, $\tan \psi = r_p/r_s$ and (ii) $\Delta = \delta_p - \delta_s$ where r_p and r_s are the Fresnel reflection coefficients for light vibrating in and perpendicular to the plane of incidence; and δ_p and δ_s are the phase shifts of these same two components brought about by reflection. Using Maxwell's equations and the appropriate boundary conditions, Drude obtained a general equation now known as the "exact equation" which is given below

$$\tan \psi \, e^{i\Delta} = \frac{r_{1p} + r_{2p} \, e^{-2i\delta}}{1 + r_{1p} r_{2p} \, e^{-2i\delta}} \times \frac{1 + r_{1s} r_{2s} \, e^{-2i\delta}}{r_{1s} + r_{2s} \, e^{-2i\delta}} \qquad (1.1)$$

where r_{1p}, r_{1s} = Fresnel coefficients for reflection at the film from the first medium (Fig. 1) for the parallel and the perpendicular components respectively

r_{2p}, r_{2s} = Fresnel coefficients for reflection at the film-substrate interface for the parallel and the perpendicular components respectively.

$$\delta = 2n_1 \pi \cos \phi_1 \frac{d}{\lambda}$$

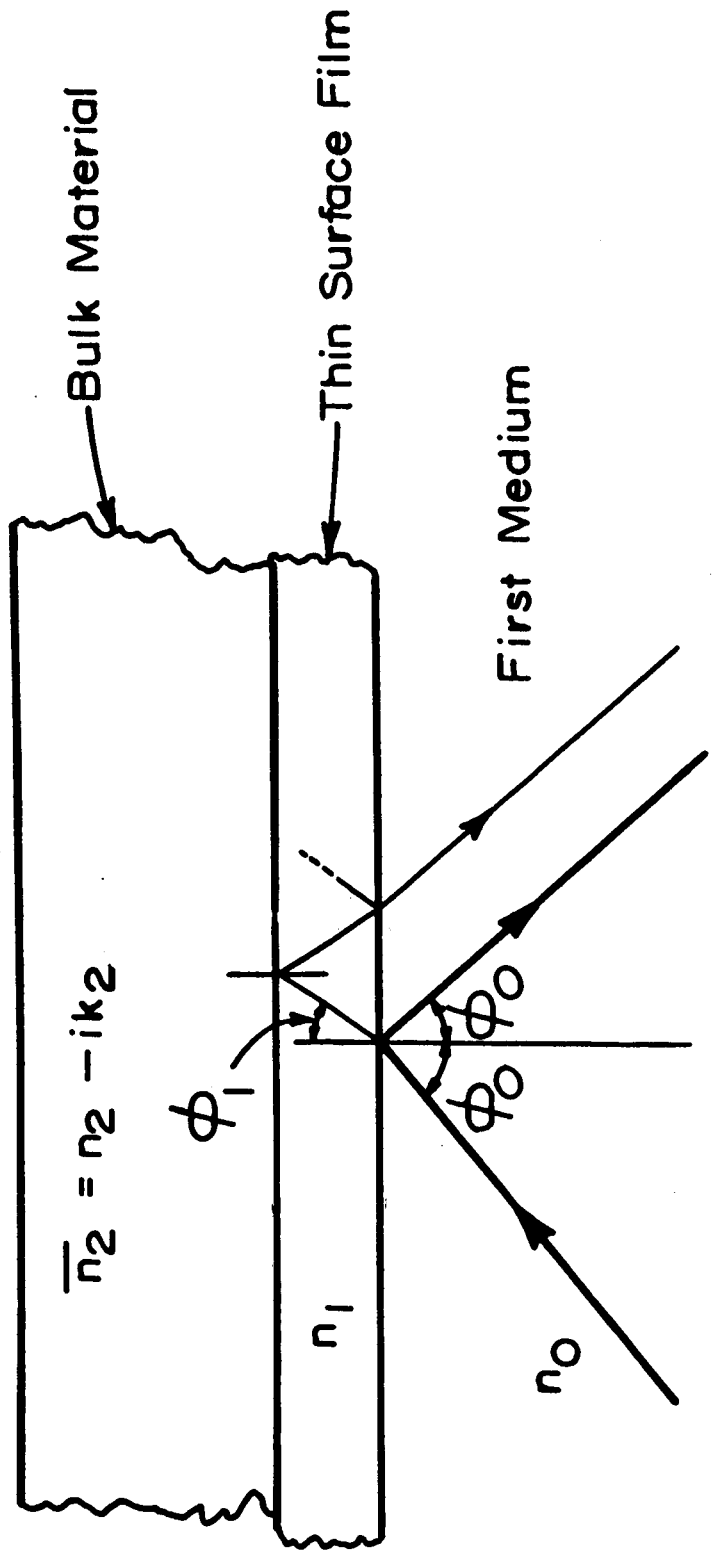

Fig. 1. Schematic representation of light from a thin surface film on an absorbing substrate

where d = thickness of the film

ϕ_1 = angle of refraction (Fig. 1)

n_1 = the refractive index of the film

λ = the wavelength of light

It should be remembered that the values of Δ and ψ can be obtained experimentally from ellipsometric measurements.

For extremely thin films ($d << \lambda$), Drude further developed his theory by expanding the term $e^{-2i\delta}$ in a series and using only the first term. These equations are referred to as Drude's approximate equations in literature and after some rearrangement they can be written as

$$\Delta - \Delta_0 = -A \left(1 - \frac{1}{n_1^2}\right) \frac{d}{\lambda}$$

$$2\psi - 2\psi_0 = B \left(1 - C\right)\left(1 - \frac{1}{n_1^2}\right) \frac{d}{\lambda} \qquad (1.2)$$

where Δ_0 and ψ_0 refer to the values obtained for a film free surface. In these equations, A and B are functions of the angle of incidence and the optical constants of the substrate and $C = n_1^2 \cos \phi_0$ where n_1 and ϕ_0 have been defined before.

Since then numerous investigators[2,3,4,5] have derived various approximate equations relating Δ and ψ to the film thickness and its refractive index. However, recently Saxena[3] has considered the errors involved in using such linear approximations of the exact equation (1.1) and has shown clearly that for accurate studies of thin films, the exact equation must always be used.

Although Drude's theory and the equation (1.1) are exact, this equation cannot be solved in a closed form for the refractive index and thickness of the film in terms of the measured quantities Δ and ψ. This has been the reason why the exact equation has not been used until recently. With the advent of modern electronic computers, the use of the exact equation is routine, once the initial "programming" is complete.

General Statement of the Problem

It is well known that the surface of a freshly cleaved silicon gets contaminated in a fraction of a second on exposure to the atmospheric air, and this layer, presumably silicon dioxide on silicon affects the various properties such as work function, surface conductance, photo-conductance, surface recombination velocity, low energy electron diffraction, etc. Numerous articles have appeared on this topic and on the various ways by which this surface effect can be diminished or in some circumstances controlled. On the other hand, the number of papers that have appeared on the nature and the exact constituents of the contaminant layer on the surface are small. Moreover, the results obtained have been sketchy and far from satisfactory.

It is possible to uniquely determine the refractive index and the thickness of the contaminant film by ellipsometric measurements provided the thickness of the film is rather large ($d > 250$ Å). However, when d is small (i.e. < 250 Å), all the curves of Δ and ψ plotted as a function of film thickness for various values of

refractive index of the film overlap. Hence, from the experimental values of Δ and ψ, it has not been possible to calculate d and n_1 independently. In order to calculate d, n_1 must be known beforehand. This fact can be appreciated more on referring to Fig. 2 where the overlap of the curves is shown for measurements with air as the first medium, as has been the practice thus far. In this curve $\delta = 1°$ corresponds to 13.6 Å.

Further, it is not known so far whether the refractive index itself depends on thickness or not, especially when the film thickness is small, since the bulk properties of the material need not necessarily hold at small film thicknesses.

In the case of silicon[5] the refractive index of the oxide film is usually taken to be 1.460 for λ5461 Å. This corresponds to the refractive index of vitreous silica. There is no evidence to indicate that the oxide film is in such disordered state for small film thicknesses. As ordered forms of silicon dioxide stable at room temperature (e.g. α-quartz, cristobalite, etc.) have slightly higher refractive indices than vitreous silica, a direct determination of the refractive index of the film should provide some information about the degree of order at such small film thickness. Further if the value of the refractive index for different film thicknesses can be determined, then it will be of interest to see how it varies with film thickness.

One possible way of determining the refractive index and the thickness of the film independently is to employ two different fluids as the first medium (e.g. air and an inert liquid like benzene, or

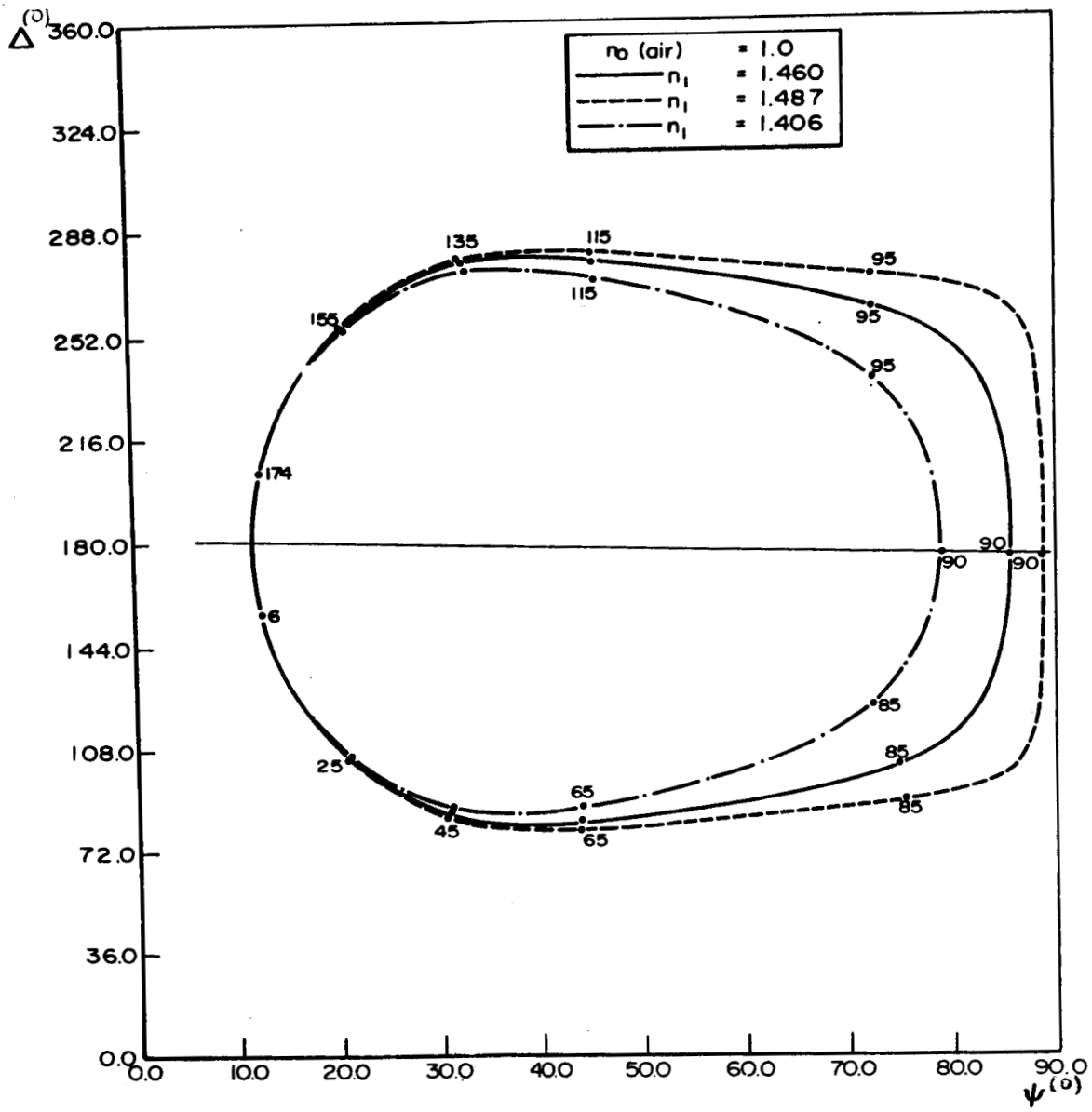

Fig. 2. Variation of Δ and ψ with δ for the light incident from air (The numerical values on the curves represent the values of δ in degrees at that point)

toluene, or carbon tetrachloride, etc.) and solve for the two variables--refractive index and film thickness.

Specific Statement of the Problem

It is proposed to determine the thickness and the refractive index of a thin oxide film on silicon, by allowing light to be incident on the film from liquids like toluene, benzene, etc. Two cases arise:

1. the index of refraction of the liquid is smaller than the index of refraction of the film (i.e. $n_0 < n_1$) or
2. the index of refraction of the liquid is greater than the index of refraction of the film (i.e. $n_0 > n_1$). Two subcases arise here:
   a. the angle of incidence is less than the critical angle (i.e. $\phi_0 < \phi_c$) or
   b. the angle of incidence is greater than the critical angle (i.e. $\phi_0 > \phi_c$)

Both the cases (1) $n_0 < n_1$ and (2a) $\phi_0 < \phi_c$ can be studied by using the exact equation of Drude and with the help of a suitable computer program to solve the exact equation.

Case (2b) $\phi_0 > \phi_c$ has not been studied theoretically until now for a substrate having a complex index of refraction. Vasicek[6] has considered this problem when the substrate is a nonabsorbing dielectric medium like glass. A completely new set of equations have to be derived starting from Fresnel relations, and a suitable computer program has to be written for this case.

It is proposed to investigate whether such a procedure will lead to increased sensitivity in the determination of the refractive index and thickness. Further it is proposed to utilize the above results to explore the possibility of finding a suitable procedure of simultaneously determining the refractive index and the thickness of thin films.

As far as the author is aware, such studies have not been reported thus far.

Scope and Limitations of the Present Studies

The technique for studying thin films by allowing light to fall from a medium of refractive index greater than the film refractive index is a powerful tool which is described in the later chapters of this thesis. This technique can be used for many other thin films besides the case of SiO_2 film on Si discussed here. One serious limitation of the method however, is in the assumption that the liquid does not contaminate the "clean" surface nor interact with the film when once it is formed. This is not an unreasonable assumption especially when inert oxygen free organic liquids like benzene, toulene, etc. are used for such studies. It has been shown that the surface sensitive mechanical properties of clean surfaces of LiF, NaF and CaF_2 are not affected by these inert liquids, at least during the time interval of these measurements.[16]

II. THEORETICAL

The theoretical studies conducted, for the various cases mentioned in the previous chapter, are given in detail in the next few pages. The fixed constants used are:

wavelength of light, $\lambda = 5461$ Å

index of refraction of silicon, $\bar{n}_2 = (4.050\text{-}0.028i)$ [7]

angle of incidence, $\phi_0 = 70.0°$, unless stated otherwise

A computer program has been written for all the cases where suitable expressions for Δ and ψ were available. The case where mathematical expressions for Δ and ψ were not available, they were derived before writing the program.

Measurements in Air

In this case the well-known Drude's exact equations for the ellipticity parameters of the reflected light are valid. For the sake of completeness these equations are given below.

$$\tan \psi \, e^{i\Delta} = \frac{r_{1p} + r_{2p} \, e^{-2i\delta}}{1 + r_{1p} r_{2p} \, e^{-2i\delta}} \quad \frac{1 + r_{1s} r_{2s} \, e^{-2i\delta}}{r_{1s} + r_{2s} \, e^{-2i\delta}} \qquad (2.1)$$

where ψ and Δ are the ellipticity parameters, r_{1p}, r_{2p}, r_{1s}, and r_{2s} are the Fresnel reflection coefficient for the parallel (p) and perpendicular (s) components at the interfaces 1 and 2 shown in

Fig. 1. The expressions for these Fresnel coefficients are given below:

$$r_{1p} = (n_0 \cos \phi_1 - n_1 \cos \phi_0)/(n_0 \cos \phi_1 + n_1 \cos \phi_0)$$

$$r_{1s} = (n_0 \cos \phi_0 - n_1 \cos \phi_1)/(n_0 \cos \phi_0 + n_1 \cos \phi_1) \qquad (2.2)$$

$$r_{2p} = (n_1 \cos \bar{\phi}_2 - \bar{n}_2 \cos \phi_1)/(n_1 \cos \bar{\phi}_2 + \bar{n}_2 \cos \phi_1)$$

$$r_{2s} = (n_1 \cos \phi_1 - \bar{n}_2 \cos \bar{\phi}_2)/(n_1 \cos \phi_1 + \bar{n}_2 \cos \bar{\phi}_2)$$

ϕ_1 is the angle of refraction in the film and $\bar{\phi}_2$ is given by

$$\bar{n}_2 \cos \bar{\phi}_2 = (\bar{n}_2^2 - n_1^2 \sin^2 \phi_1)^{1/2} \qquad (2.3)$$

δ is related to the thickness d of the film by the following equation

$$\delta = \frac{2\pi d}{\lambda} (n_1^2 - n_0^2 \sin^2 \phi_0)^{1/2} \qquad (2.4)$$

where λ is the wavelength of light.

The program given in Appendix A was used to obtain the values of Δ and ψ at close intervals of δ for various assumed values of the refractive indices of the film. In this program the value of RNXA (i.e. n_0) was taken to be unity, the value of the refractive index of air. Figure 2 shows the variation of Δ and ψ as a function of δ when light is incident from air on to films with refractive indices 1.406, 1.460 and 1.487 on a substrate of silicon. This case has been discussed in detail by Archer[7] and Saxena,[3] and has been reported here for comparison with the results reported later in the thesis. Since the refractive index of air is less than that of the

film, there is a phase change of 180° in one of the components of the reflected light. This is the reason for plotting Δ around 180° in this case.

Measurements with Liquids

$n_0 < n_1$

When the index of refraction of the liquid is smaller than the index of refraction of the film, the equations mentioned in the case of measurements in air can be used and a similar analysis carried out using the appropriate value of the refractive index of the liquid for RNXA.

$n_0 > n_1$

In such a case, two situations are possible: Case (1) the angle of incidence ϕ_0 is less than the critical angle ϕ_c ($= \sin^{-1} n_1/n_0$) and Case (2) $\phi_0 > \phi_c$. For both these cases detailed calculations have been carried out and the results are discussed below.

Reddy and Bokris[17] used a liquid (an electrolyte) as the first medium in their electrochemical studies; but in their case the refractive index of the first medium was less than that of the film and hence they could employ the well-known equations of Archer.[2]

The case where the first medium has a higher refractive index than the film has also been considered by Passaglia et al.,[8] but in their studies, the substrate was nonabsorbing.

Case (1), $\phi_0 < \phi_c$: Here again, the well-known equations of Drude (2.1 to 2.4) are valid. Using these equations, detailed computations of Δ and ψ have been made with IBM 7074 Computer using the program given in Appendix A. Of course, in this case, the symbol RNXA used in the program indicates the refractive index of the liquid. It should be noted that the values of the refractive indices of the film n_1 for which computations can be carried out is limited by the condition $n_1 \geq n_0 \cdot \sin \phi_0$.

Figure 3 shows the variation of Δ and ψ for δ varying from 0° to 180° for the case of light incident from the liquid toluene (n_1 = 1.496 for λ5461 Å) on to surface films of refractive indices 1.487, 1.460 and 1.406; on the substrate silicon. The first two values chosen for the refractive index of the film correspond to the index of cristobalite and vitreous silica respectively. The value 1.406 for the refractive index of the film corresponds to a critical angle slightly larger than the angle of incidence of 70° used in the calculations. Representative values of δ are marked on the curves.

The most striking result which is apparent on a study of the figure is the very large change in Δ and an appreciable change in ψ for small changes in δ as the angle of incidence approaches the critical angle. For example for the highest refractive index of the film used in the calculation 1.487, Δ changes from 7.65° at δ = 0 to -20.27° at δ = 32°. While for the smallest refractive index of film, 1.406 (i.e. when the critical angle is only slightly larger than the angle of incidence) Δ changes from 7.65° at δ = 0 to -56.12° at δ = 0.50°.

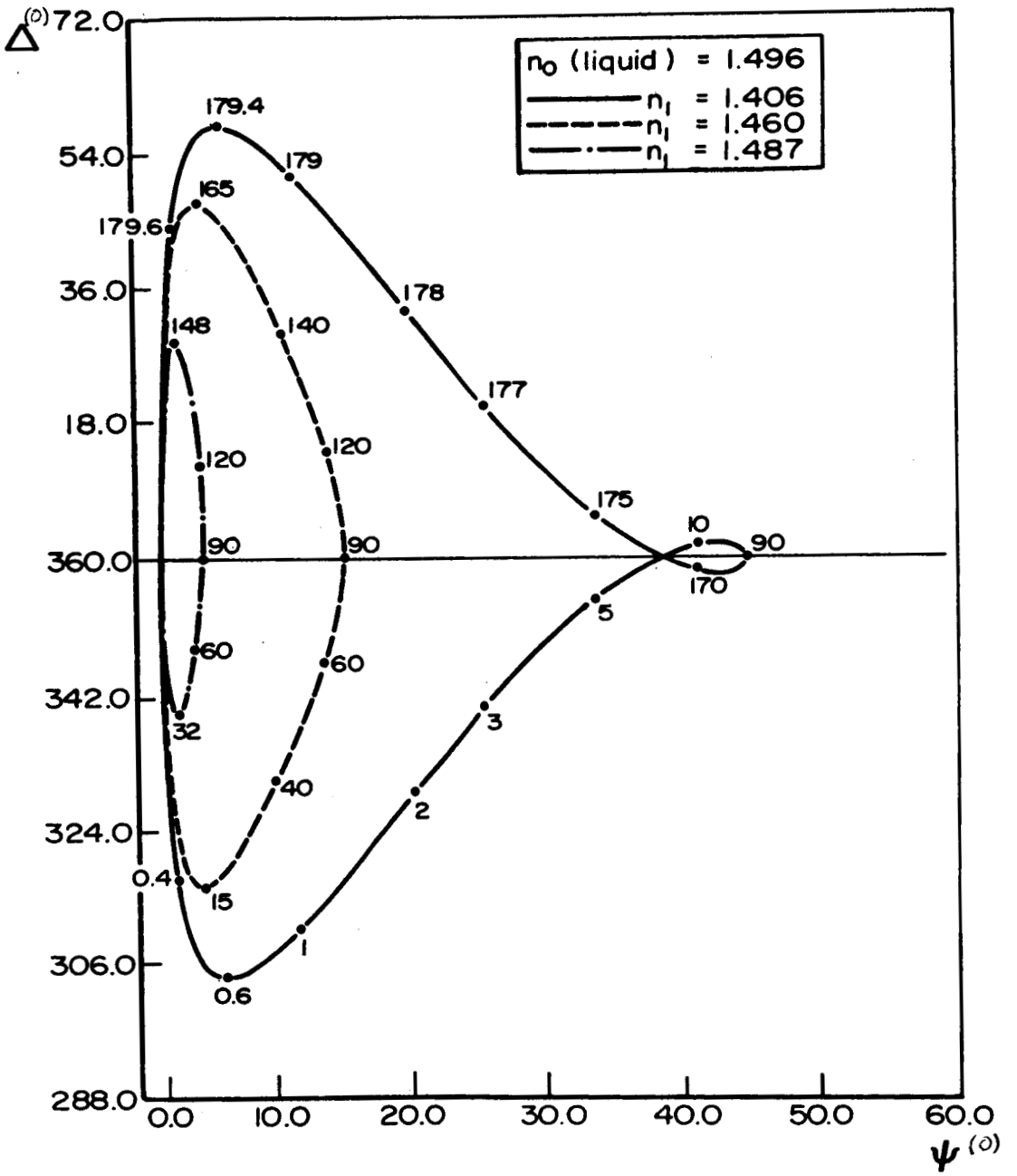

Fig. 3. Variation of Δ and ψ with δ for the light incident from toluene (The numerical values on the curves represent the values of δ in degrees at that point)

The apparent highly increased sensitivity with respect to δ when using a liquid of suitable refractive index instead of air as the first medium is, however, very deceptive. This can be seen from Table 1, where the film thickness and the changes in Δ corresponding to value of $\delta = 0.10$ are given for various liquids. As one approaches the critical angle, $(n_1^2 - n_0^2 \sin^2 \phi_0)$ tends to zero and hence it is seen from equation (2.4) that a small value of δ corresponds to a large value of d. Thus it appears that the sensitivity with respect to the film thickness is about the same whatever be the first medium.

Figure 4 exhibits the variation of Δ and ψ as a function of δ for three different values of the refractive index of the liquid. The angle of incidence is again assumed to be 70° and the refractive index of the film on a substrate of silicon is assumed to be 1.460. The refractive indices 1.467 and 1.496 for the liquid correspond to that of carbon tetrachloride and toluene respectively. The value 1.5536 for the refractive index of the liquid corresponds to a critical angle slightly larger than 70°. The curves again show the same features as described in the previous paragraph.

Case (2), $\phi_0 > \phi_c$: When the angle of incidence ϕ_0 is greater than the critical angle ϕ_c, total reflection takes place at the liquid-film interface. However, a disturbance is propagated inside the film and this decays exponentially. For very small film thicknesses one would expect this disturbance to be reflected from the interface between the film and the substrate and affect the values of Δ and ψ.

Table 1

Values of $(\Delta - \Delta_0)$ and d in the Three Systems: air, CCl_4 and $C_6H_5CH_3$

$n_1 = 1.460$		$\phi_0 = 70°$	$\delta = 0.10$
	n_0	$\Delta - \Delta_0$ (in degrees)	d in Å
air	1.000	0.42	1.36
CCl_4	1.4671	0.21	3.16
$C_6H_5CH_3$	1.4960	0.80	3.85
-	1.5536	27.61	89.5

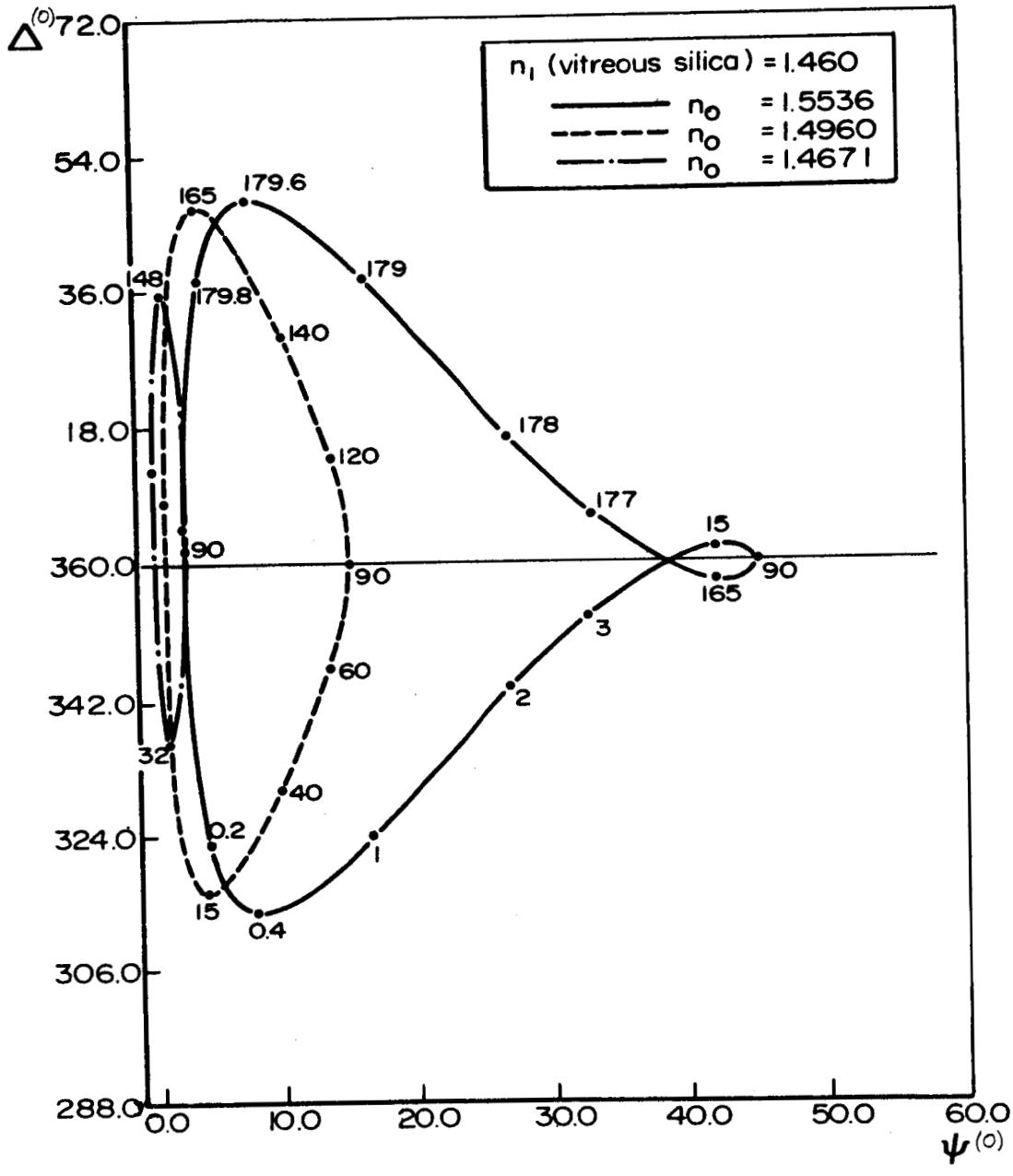

Fig. 4. Variation of Δ and ψ with δ for the light incident on a vitreous silica film on silicon (The numerical values on the curves represent the values of δ in degrees at that point)

Vasicek[6] has considered this problem for the case when the substrate is a nonabsorbing dielectric medium like glass. But for an absorbing substrate like silicon, the results will be different. Suitable expressions for Δ and ψ have been derived for such a case as shown below.

Let us consider light incident from a medium of refractive index n_0 on to a film of refractive index n_1 and let this film lie on a substrate of complex refractive index $\bar{n}_2$. If $n_0 > n_1$, and the angle of incidence ϕ_0 greater than the critical angle ϕ_c, then the reflection coefficients at the first boundary are

$$r'_p = e^{i\delta'_p} \tag{2.5}$$

$$r'_s = e^{i\delta'_s} \tag{2.6}$$

where δ'_p and δ'_s are given by

$$\tan 1/2\delta'_s = (n_0^2 \sin^2 \Phi_0 - n_1^2)^{1/2}/n_0 \cos \phi_0 \tag{2.7}$$

and

$$\tan 1/2\delta'_p = \frac{n_0^2}{n_1^2} \tan 1/2\delta'_s \tag{2.8}$$

We have to use the Fresnel's formulae

$$r_p e^{i\delta_p} = \frac{r'_p + r''_p e^{-ix}}{1 + r'_p r''_p e^{-ix}} \tag{2.9}$$

$$r_s e^{i\delta_s} = \frac{r'_s + r''_s e^{-ix}}{1 + r'_s r''_s e^{-ix}} \tag{2.10}$$

where

$$x = \frac{4\pi d}{\lambda} (n_1^2 - n_0^2 \sin^2 \phi_0)^{1/2} = -i\delta' \tag{2.11}$$

To calculate r_p'' and r_s'' let us take the limiting case, $x = 0$.

In this case the medium of refractive index n_0 is in direct contact with medium of complex refractive index $\bar{n}_2$ and the reflection coefficients $r_p^o e^{i\delta_p^o}$ and $r_s^o e^{i\delta_s^o}$ are given by

$$r_p^o e^{i\delta_p^o} = \frac{\bar{n}_2 \cos \Phi_0 - n_0 \cos \bar{\Phi}_2}{\bar{n}_2 \cos \Phi_0 + n_0 \cos \bar{\Phi}_2} \tag{2.12}$$

$$r_s^o e^{i\delta_s^o} = \frac{n_0 \cos \Phi_0 - \bar{n}_2 \cos \bar{\Phi}_2}{n_0 \cos \Phi_0 + \bar{n}_2 \cos \bar{\Phi}_2} \tag{2.13}$$

$$\bar{n}_2 \cos \bar{\Phi}_2 = (\bar{n}_2^2 - n_0^2 \sin^2 \Phi_0)^{1/2} \tag{2.14}$$

Hence

$$r_p^o e^{i\delta_p^o} = \frac{e^{i\delta_p'} + r_p''}{1 + e^{i\delta_p'} r_p''} \tag{2.15}$$

Hence

$$r_p'' \left[r_p^o e^{i(\delta_p^o + \delta_p')} - 1 \right] = e^{i\delta_p'} - r_p^o e^{i\delta_p^o} \tag{2.16}$$

$$r_p'' = -e^{i\delta_p'} \frac{\left[1 - r_p^o e^{i(\delta_p^o - \delta_p')}\right]}{\left[1 - r_p^o e^{i(\delta_p^o + \delta_p')}\right]} \tag{2.17}$$

Similarly for r_s''

$$r_s'' = -e^{i\delta_s'}\left[\frac{1 - r_s^o e^{i(\delta_s^o - \delta_s')}}{1 - r_s^o e^{i(\delta_s^o + \delta_s')}}\right] \tag{2.18}$$

Now for an arbitrary thickness d of film,

$$r_p e^{i\delta_p} = \frac{e^{i\delta_p'} - e^{i\delta_p'}\dfrac{\left[1 - r_p^o e^{i(\delta_p^o - \delta_p')}\right]e^{-ix}}{\left[1 - r_p^o e^{i(\delta_p^o + \delta_p')}\right]}}{1 - e^{i\delta_p'}e^{i\delta_p'}\dfrac{\left[1 - r_p^o e^{i(\delta_p^o - \delta_p')}\right]e^{-ix}}{\left[1 - r_p^o e^{i(\delta_p^o + \delta_p')}\right]}} \tag{2.19}$$

or

$$r_p e^{i\delta_p} = \frac{e^{i\delta_p'}\left[(1-r_p^o 1\ \mathrm{expi}(\delta_p^o+\delta_p')) - e^{-\delta'}(1-r_p^o\ \mathrm{expi}(\delta_p^o-\delta_p'))\right]}{\left[1 - r_p^o e^{i(\delta_p^o + \delta_p')}\right] - e^{-\delta'}\left[1 - r_p^o e^{i(\delta_p^o - \delta_p')}\right] e^{i2\delta_p'}} \tag{2.20}$$

Similarly

$$r_s e^{i\delta_s} = \frac{e^{i\delta_s'}\left[(1-r_s^o\ \mathrm{expi}(\delta_s^o+\delta_s')) - e^{-\delta'}\ (1-r_s^o\ \mathrm{expi}(\delta_s^o-\delta_s'))\right]}{\left[1 - r_s^o e^{i(\delta_s^o + \delta_s')}\right] - e^{-\delta'}\left[1 - r_p^o e^{i(\delta_s^o - \delta_s')}\right] e^{i2\delta_s'}} \tag{2.21}$$

Since

$$\tan\Psi\, e^{i\Delta} = \frac{r_p}{r_s}\, e^{i(\delta_p - \delta_s)} \tag{2.22}$$

one can evaluate ψ and Δ from equations (20, 21, 22). Such computations have been performed with the help of IBM 7074 computer (see program write up in Appendix B) and the results obtained are discussed below.

Figure 5 shows the variation of Δ as a function of δ' for various angles of incidence beyond the critical angle, for light incident from toluene with a refractive index 1.496 on to a film of refractive index 1.460 on silicon. Finally Fig. 6 shows the variation of Δ as a function of δ' for an angle of incidence 89°, the liquid medium being toluene. In this case the films on the silicon surface have different refractive indices varying from 1.100 to 1.460. In Figs. 5 and 6 the region of δ' from 0 to 40° is shown on an enlarged scale. The main conclusions to be drawn from a study of these figures are:

(i) The overall sensitivity in this technique is very poor compared to that when the angle of incidence ϕ_0 is less than the critical angle ϕ_c.

(ii) All the change in Δ takes place for δ' less than 80°. For larger values of δ', in other words for larger thickness of the films, there is almost no change in Δ. This would be expected since in the phenomenon of total internal reflection the disturbance which penetrates the film decays exponentially and hence increasing the film thickness beyond a certain value will have no effect.

(iii) A study of Fig. 6 reveals a decrease in sensitivity with increasing critical angle.

(iv) As the angle of incidence is increased from the critical angle the sensitivity increases initially, and then starts to decrease. This is seen in Fig. 5.

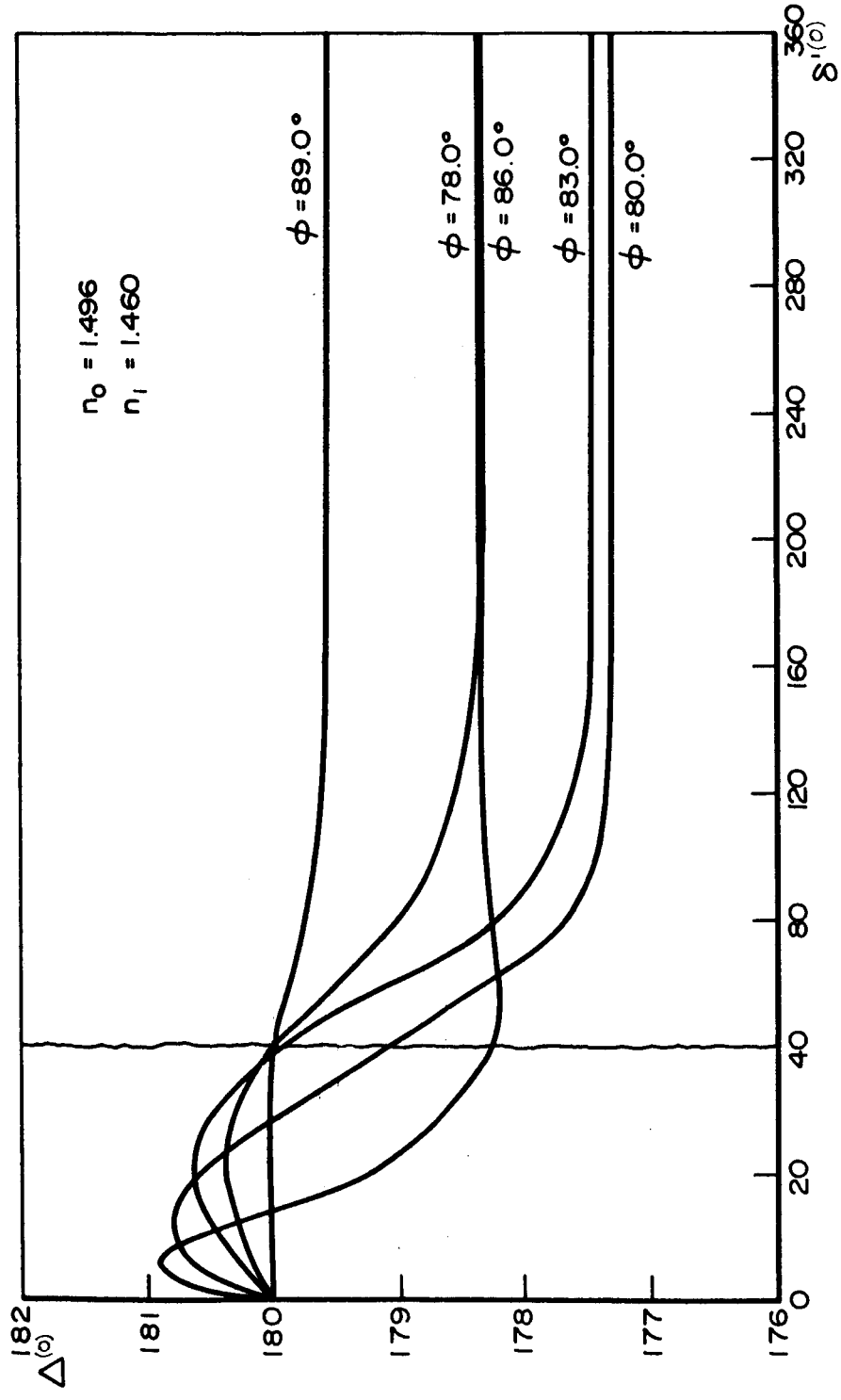

Fig. 5. Variation of Δ with δ' for various angles of incidence higher than the critical angle, from toluene on to vitreous silica film on silicon

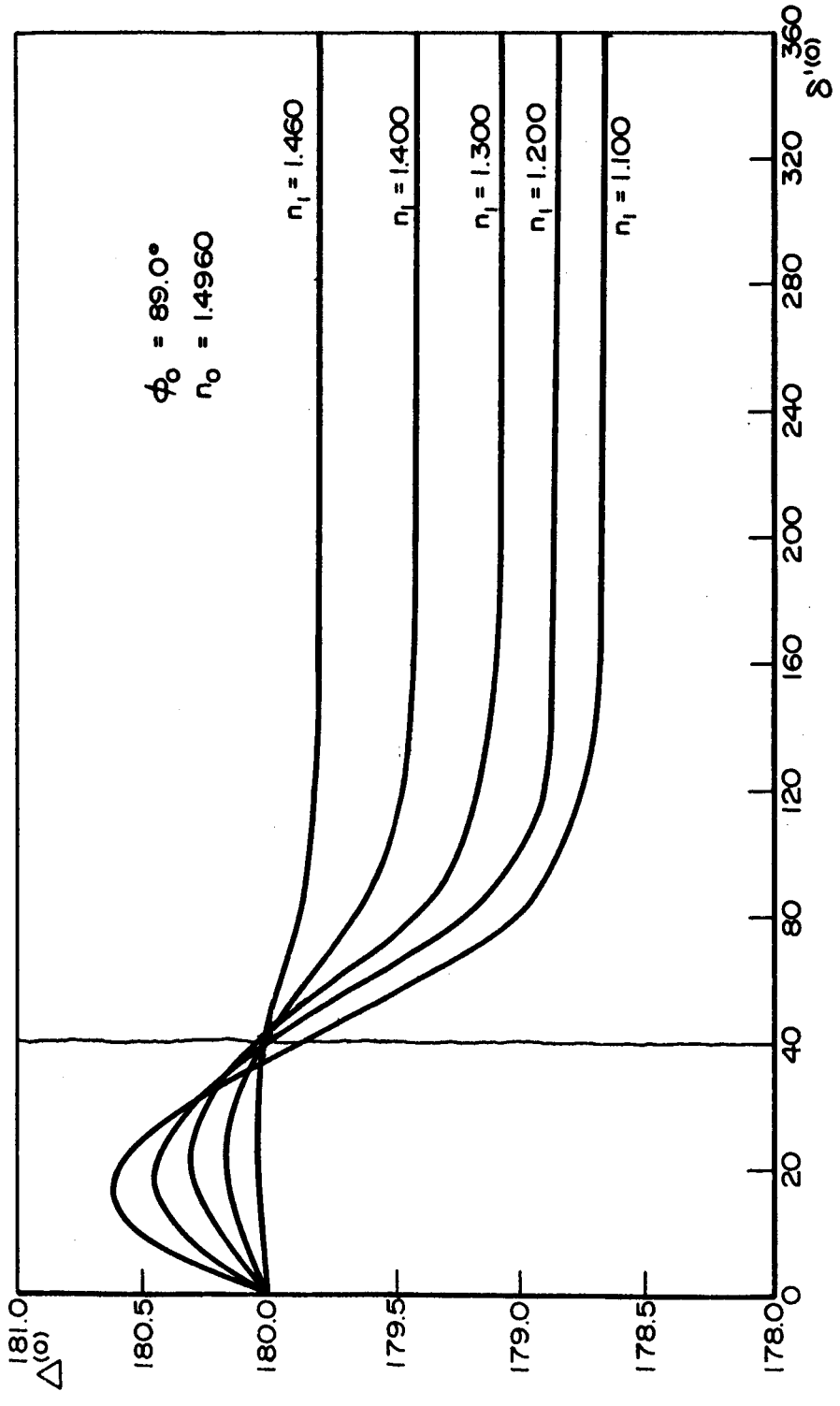

Fig. 6. Variation of Δ with δ' at an angle of incidence 89° from toluene on to various films on silicon

The final conclusion from these studies is that it is not advantageous to work with angles of incidence greater than the critical angle.

Conclusions

From these theoretical studies it can be concluded that in ellipsometry, light can be allowed to be incident from a dense medium like a liquid on to a film over an absorbing substrate. In such a case two basic situations arise: (i) when the angle of incidence ϕ_0 is less than the critical angle ϕ_c and (ii) when $\phi_0 > \phi_c$. It is further concluded from the detailed calculations that the sensitivity with which the thickness of the film with an assumed refractive index can be measured is nearly the same whatever be the first medium for case (i) but in the case (ii) the sensitivity is very poor.

III. INSTRUMENTATION

The instrumentation to be used with the ellipsometer was developed keeping in mind that the same instrumentation could be used in the studies of kinetics of oxidation of silicon in the initial rapid oxidation region where measurements have to be made in vacuum.

It is well known that the surfaces of a freshly cleaved sample of any material, e.g. like a silicon single crystal get contaminated by oxygen and other constituents of the atmospheric air within a fraction of a second. Further, even in the best vacuum available in the laboratory noticeable contamination of such a "clean" surface by oxygen can be detected in a matter of minutes. Hence in studies such as the oxidation kinetics of "clean" surfaces it is imperative that the method of measurement must satisfy both the following conditions: (i) the measuring technique itself should not influence the property being studied and (ii) the time taken to complete one measurement at any stage must be very small--at least of the order of a second if not less. The ellipsometric technique can be conveniently used for these type of studies, provided the second condition is satisfied. The following describes an experimental arrangement by which this has been achieved at a relatively moderate cost. As far as the author is aware, such a system or any arrangement similar to this has not been described in the literature.

Since the experimental arrangement is almost identical for polarimetric measurements, the same procedure can be adapted to advantage to study the time dependence of the optical rotatory power of mutarotatory materials and such other phenomena which are strongly time dependent.

Experimental Technique

The principle as well as the basic instrumentation of ellipsometry is well known and has been described in numerous publications.[9,10] Figure 7 is a schematic representation of the experimental set up used in ellipsometric measurements. To recapitulate briefly the ellipsometer is a standard polarizing spectrometer with the facility to introduce a quarter wave plate in the optical path either before or after reflection from the experimental surface. Consider the former case, i.e. the quarter wave plate transmits the incident beam and that it is fixed in orientation with the fast axis inclined at 45° to the plane of incidence. In such a case when the polarizer and analyzer are suitably oriented so that the beam reflected from the surface is extinguished by the analyzer, then it can be shown[11] that

$$\Delta = 90° - 2P$$

and

$$\psi = -A$$

where Δ and ψ are the ellipticity parameters which define the ratio of the Fresnel coefficients for the p and s component waves i.e.,

$$\frac{r_p}{r_s} = \tan \psi \, e^{i\Delta}$$

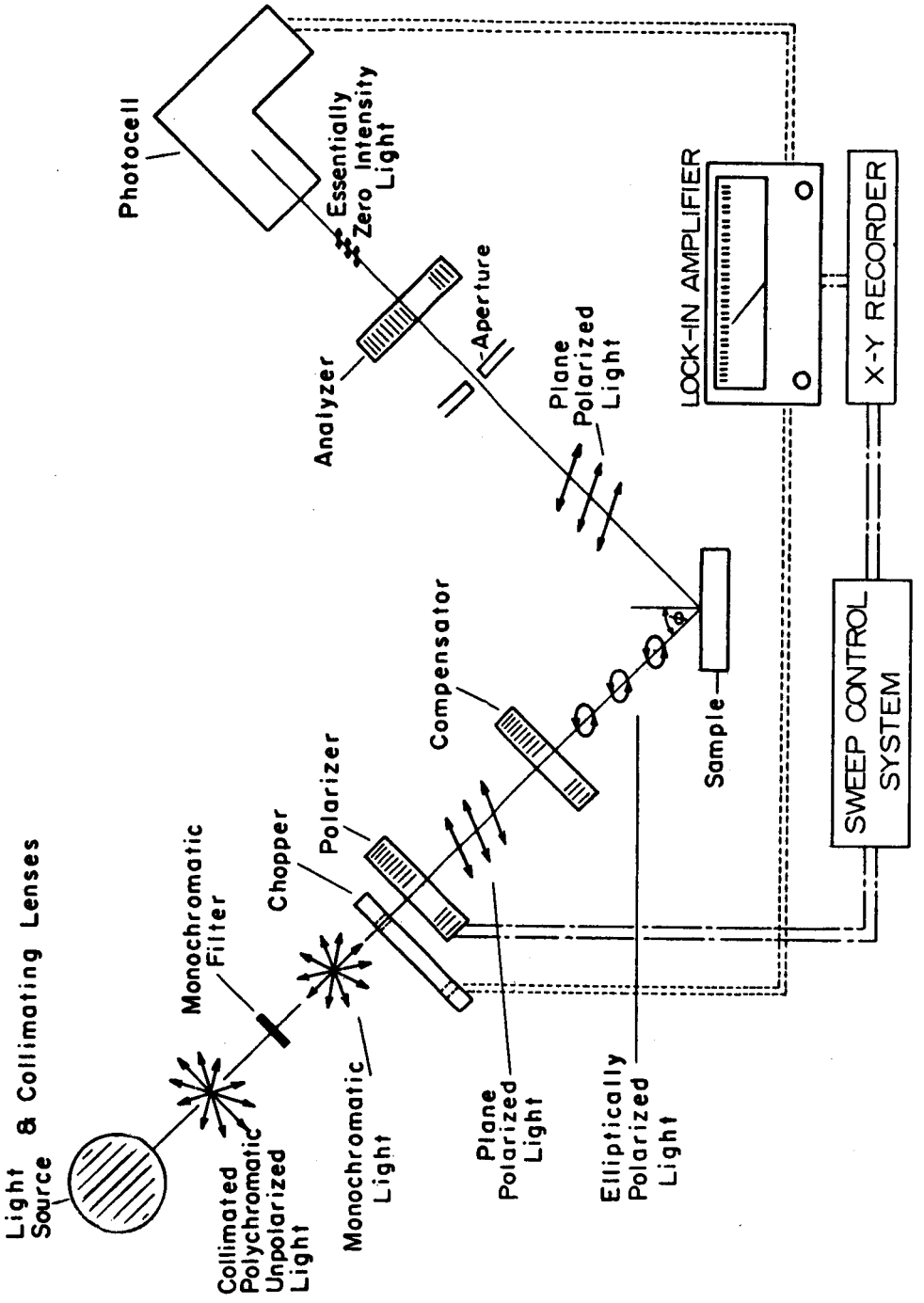

Fig. 7. Schematic drawing of ellipsometry

and P and A are the orientations of the polarizer and analyzer at extinction.

Further it is usually found that only one of these two ellipticity parameters vary significantly while the second remains essentially constant during the course of an experiment of short duration. For example in the case of the formation of SiO_2 over Si in air, during the time Δ varied by 2°, the variation in ψ was only 0.01°. Thus in this case one can follow the formation of the contaminating oxide layer on the surface of silicon by following the changes in Δ keeping ψ constant; in other words in this experiment it is only necessary to change the position of polarizer P keeping the analyzer A fixed, to obtain good extinction. Of course, when large thickness variations of the contaminating layer are considered, it will be necessary to vary both Δ and ψ. However in such cases the time interval is usually much larger and thus it is not necessary to employ a rapid determination technique.

Details of Instrumentation

In the experimental setup developed shown schematically in Fig. 8 the light source is a high intensity PEK #110 d.c. mercury arc lamp with a luminous intensity of approximately 14,000 candles/cm^2. A PEK Model 401 power supply provides the necessary operating voltage and current for the lamp. The a.c. ripple on the output of the 401 power supply was measured to be less than 3% of the d.c. voltage at the rated load. A better regulated power supply would be advantageous in reducing the a.c. ripple noise. However,

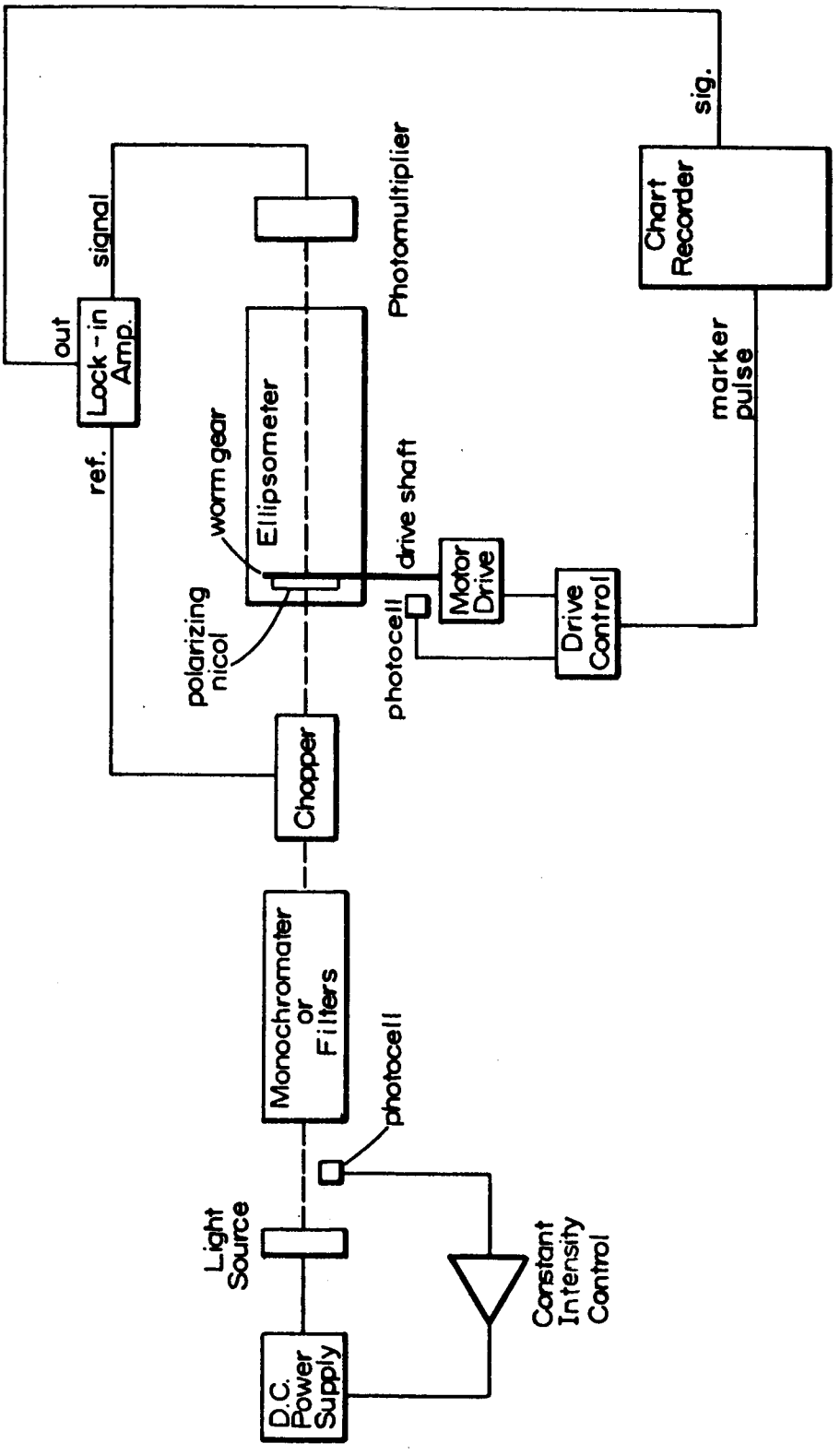

Fig. 8. Schematic block diagram of ellipsometer instrumentation

the major problem with the lamp is an intensity drift which required the necessity to adjust the power supply for constant current every 1/2 hour. An operational feed back control may prove useful in eliminating this drift, but such a control has not been employed in the setup shown. The lamp itself is mounted in a PEK Model 910 lamp housing which provides a variable-focus (12"-30") projection lens system. The lens is adjusted to obtain nearly parallel light output in the green spectral region.

The light output passes through a Fabry-Perot transmission type second-order interference filter for λ5461 Å. Since the light source is a high pressure mercury arc, there is noticeable continuous background particularly the third order transmission of the interference filter in the region at 3780 Å. Since this background in the near ultraviolet is transmitted by the interference filter, it was necessary to remove it by using a broad band yellow transmitting filter to obtain accurate values of the ellipticity parameters.

The light is then chopped by a mechanical chopper. Selection of the chopping frequency should involve the consideration of the amplifying device. Amplifiers have a noise power spectrum that varies as the reciprocal of the frequency near zero frequency due to the so-called flicker effect (1/f noise). To avoid the 1/f noise, the signal should have the frequency above 10hz for tube-type amplifiers and above 500hz for transistor systems. The chopper employed in the setup shown is a Princeton Applied Research Model BZ-1 providing an interrupting frequency of 400hz. The chopper provides an

electrically isolated square-wave signal (1 volt p-p) and this signal is used as the reference for the lock-in amplifier.

The light beam is then collimated by the entrance lens arrangement of a Gaertner ellipsometer and is linearly polarized by a Glan-Thompson prism. The standard ellipsometer unit was modified along the following lines in order that the minimum setting of the polarizer could be determined to within $\pm 0.01°$ and in a short time of the order of 1 sec. The polarizer mount is attached to a 360 tooth worm gear which is driven by a synchronous motor. One revolution of the worm rotates the worm gear (polarizer) through exactly 1°. The shaft on which the worm is mounted has a blank gear disc with a small hole through it to pass a narrow beam of light once every revolution. The beam of light hits a photocell which accuates a relay counting network (Fig. 9). The counting network provides the sweeping control by rotating the polarizer a set number of degrees, reversing direction, driving back the same number of degrees and continuing this reversing process until stopped.

Since the initial formation of the contaminating layer occurs very fast it is desirable to take as many readings as possible in a short time. The speed of the motor was selected to drive the polarizer at a rate of 1°/sec, (60 RPM). Higher speeds were tried but the major factor here is that the time constant of the lock-in amplifier must be reduced, thus increasing the effective bandwidth and the resultant noise. Also connected to the drive shaft is a 10-turn precision potentiometer. This potentiometer with a voltage divider circuit (X-axis control) is used to provide the angles of

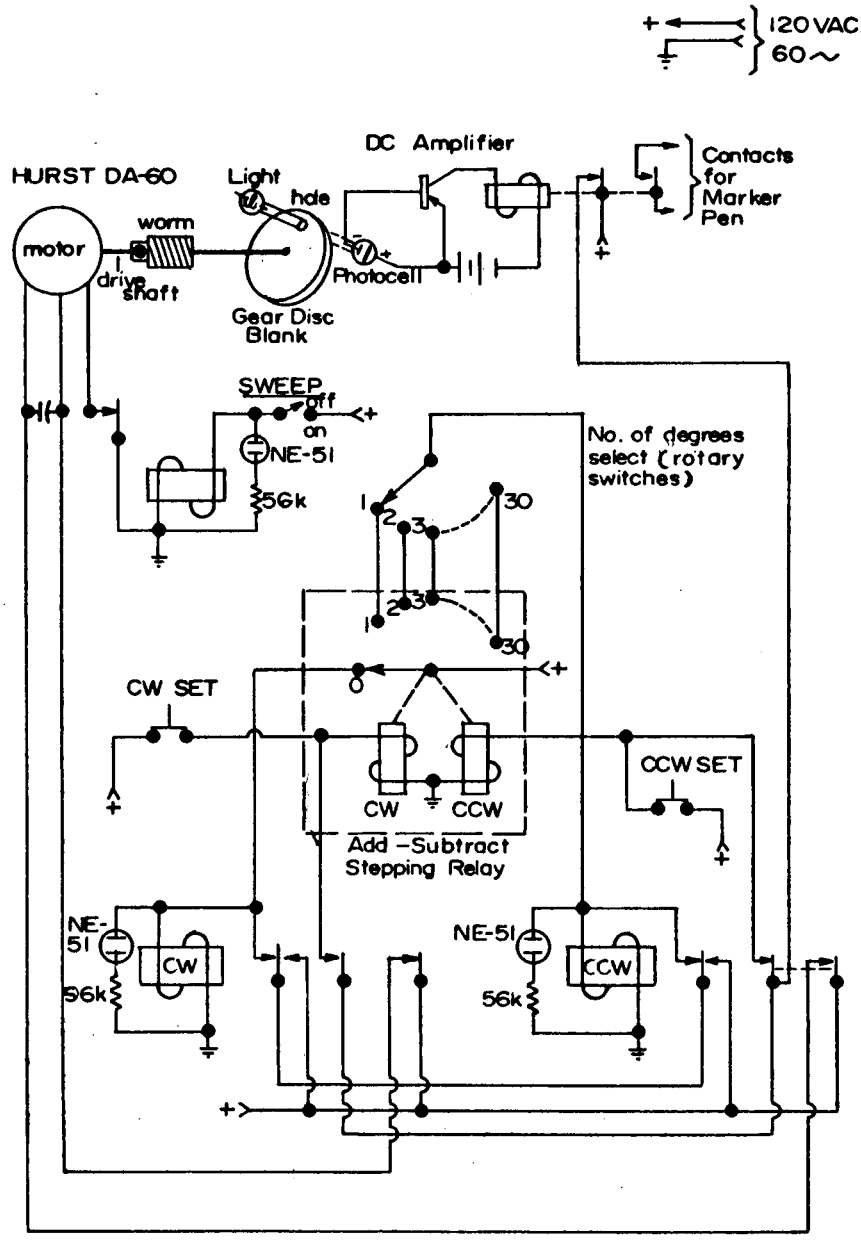

Fig. 9. Sweep control

rotation. One revolution of the shaft produces a voltage change of 10 mv at the output of the X-axis control and this output drives the X-axis of the chart recorder. Correlation of the polarizer position to the calibrations on the chart paper is made by allowing 10 mv = 1° = 1" of movement along the X-axis. A 10 mv = 1° = 2" provides higher resolution in reading accuracy of $\pm 0.01°$ or better.

If an X-Y recorder is not available, a standard roll-chart recorder can be employed by providing a marker-pulse. A chart speed of 1"/sec will provide a resolution of 1°/1". To provide accurate correlation of the marker pulses to degrees it is imperative that the motor of the sweeping drive be of the synchronous type.

Detection of the light output from the ellipsometer is done by a photomultiplier tube, the output of which is fed into the signal input of the lock-in amplifier. Stray modulated a.c. light, especially at the reference frequency of 600hz, should be effectively blocked from entering the photomultiplier since this will introduce false signals that will be detected by the lock-in amplifier. Other light, while not directly concerned with the signal, will increase the noise-in-signal due to the shot effect:

$$S/N = \frac{i}{\sqrt{i_n^2}}$$

where i_n^2 = mean shot noise current

i = average photoelectric signal current.

General considerations for improving the S/N ratio of photomultiplier detectors are

(i) The photomultiplier used should have a photocathode which shows peak sensitivity at the wavelength being used. In the setup shown, using a wavelength of λ5461 Å, a S-11 spectral response was a satisfactory choice.

(ii) Cooling the photomultiplier will reduce thermionic emission (dark current). This would be necessary if the light intensity were extremely low. It was found not necessary when using a PEK #110 mercury lamp.

(iii) Using as low a voltage on the photomultiplier tube as is consistent with the required gain. An RCA IP-21 PM tube with a supply voltage of 500-800 V and a 10 stage voltage divider of ten 25 K resistors provides a satisfactory arrangement. If the signal is very low, cooling the PM tube should be tried first rather than increasing the supply voltage.

The lock-in amplifier employed in the setup shown in Fig. 7 is a Princeton Applied Research Model JB-4. A lock-in amplifier is a detection system capable of operating with an extremely narrow equivalent noise bandwidth. The signal input is applied to a frequency selective amplifier with a $Q \simeq 25$ to limit the input bandwidth. The output of the signal amplifier is applied to the input of a phase sensitive detector which mixes the input signal and the reference signal so as to produce the corresponding sum and difference frequencies. A low-pass filter stops the upper portion of the band, but the lower side (d.c.) is passed by the low pass filter; the bandwidth of which determines the effective bandwidth of the amplifier. Lock-in amplifiers usually are called phase-sensitive

detectors because the d.c. output produced by a signal at the reference frequency is proportional to the cosine of the relative phase of the signal and the reference.

The effective integrated noise bandwidth βN_i of the amplifier is: $\beta N_i = 1/2\ RC$. If the wave shape of the signal is to be preserved the integrating time $T_i = 1/\beta N_i$ must be less than the shortest time in which a significant change in signal intensity can occur. With a time constant of 1 sec, the noise level was below 5-10 mv.

The d.c. output from the lock-in amplifier is fed into the Y-axis of an X-Y chart recorder. The output signal from the X-axis control is fed into X-axis of the recorder. The chart recorder used is a Hewlett-Packard Model 2D-2, providing an input sensitivity on both axis of as high as 0.5 mv/1". The voltage change of the Y-axis signal for a 6° sweep is approximately 400 mv. On 50 mv/inch scale the Y-axis movement is approximately 8". One possible disadvantage with an X-Y recorder is that the area of the chart is only 11" x 15", thereby limiting the number of degrees that can be recorded to 15° for 1°/1" resolution or 7° for a 1°/2" resolution. However, in the experiments on the oxidation kinetics of silicon, with air as the first medium sweeps greater than 6° have not been required.

The output graph on the chart resemble a $\cos^2\theta$ curve as can also be shown by elementary considerations of the analysis of linearly polarized light. To determine the minimum point of such a curve, the usual procedure is to select two points on either side of the minimum at which the intensities are the same, and take the mean of these two settings of the nicol. Using such a procedure an

accuracy of $\pm 0.01°$ has been achieved with air as the first medium. If the time constant is too slow, flattening of the curve will result, thus invalidating the above method of taking corresponding intensities to determine the mean position.

The advantages of this instrumentation and recording arrangement are

(i) Once approximate values of Δ and ψ are known, this method provides for a rapid scanning and a precise fixing of the extinction position.

(ii) It provides a permanent record which can be analyzed later at leisure.

IV. PRECISION CALIBRATION OF THE ELLIPSOMETER

The precision calibration of the different ellipsometer components namely the polarizer, analyzer and the quarter wave plate, was carried out as follows.

Brewster Angle Method

Monochromatic light linearly polarized was allowed to be incident on a vitreous silica plate at the angle of incidence equal to the Brewster angle (ϕ_B = 55°35' for λ5461 Å). A mercury arc with an appropriate interference filter isolating λ5461 Å was used as the light source. Since the vitreous silica behaves like a nonabsorbing dielectric material at this wavelength, the intensity of the reflected light with the component parallel to the plane of incidence is zero, provided the light is incident at the Brewster's angle. There might be a slight complication due to the fact that a thin surface film is usually present on each material preserved at room temperature in normal atmosphere. But with silica the situation is rather good from this point of view because the thickness of the surface film on vitreous silica is usually extremely low and thus it seems to be a suitable material for our purposes. It is rather easy to find the position of absolute minimum of light by rotating the polarizer. This value fixes the position of polarizer. During this

calibration of the polarizer, the analyzer and the quarter wave plate were removed from the ellipsometer. Initially the calibration was performed with the naked eye. After establishing the position of polarizer approximately the polarizing nicol is adjusted in its graduated circle such that when the plane of vibration of the polarized light is parallel to the plane of incidence the reading on the circle of polarizer corresponds to 0°. The final adjustments were carried out with the help of the photoelectric system described in Chapter III. Using the same arrangement the position of the polarizer is established. The results of this measurement is presented in Table 2 to show the accuracy of the adjustments.

It is seen that the accuracy of the setting of the position of the polarizer seems to be quite reasonable.

After thus establishing the position of the polarizer, the analyzer was put back into its own place in the ellipsometer. Keeping the position of the polarizer fixed, the analyzing nicol was adjusted to be in the "crossed" position with respect to the polarizer and the graduated circle of the analyzer was then suitably fixed. Table 3 gives the results of the checking of the final setting of the analyzer.

The accuracy of the analyzer adjustment is better than in the case of polarizer, thus indicating that the relative position of crossed polarizer and analyzer may be determined more precisely than their absolute positions with respect to the plane of incidence.

Lastly the setting of quarter wave plate was fixed as follows. The polarizer and the analyzer were first adjusted to be in the crossed position. When the quarter wave plate was introduced in the

Table 2

Calibration of the Polarizer

	P(°)	Δ_+	Δ_-	
1	187.61		0.039	
2	62		029	
3	68	0.031		
4	70	051		$\delta_p = \frac{5}{2} \frac{\Sigma\Delta_+}{n\sqrt{n-1}}$
5	60		049	
6	61		039	$= \frac{\Sigma\Delta_+}{12}$
7	69	041		
8	69	041		
9	65	001		
10	64		009	
	1876.49	0.165	0.165	

$\bar{P} = (187.64_9 \pm 0.01)°$ or $P = (187.65 \pm 0.01)°$

Table 3

Calibration of the Analyzer

	P(°)	Δ_+	Δ_-	
1	348.52	0.020		
2	51	010		
3	52	020		
4	51	010		
5	47		0.030	$\partial_A = \frac{\Sigma\Delta_+}{12}$
6	49		010	
7	49		010	
8	50			
9	51	010		
10	49		010	
	3485.01	0.070	0.060	

$\bar{A} = (348.50_1 \pm 0.006)°$ or $A = 348.51$

optical path, in general there will be a restoration of light intensity, unless one of the axes of quarter wave plate (either "fast" or "slow") coincides with either the plane of polarization of the polarizer or of the analyzer. Hence the setting of the quarter wave plate was adjusted and fixed in such a way to yield minimum intensity of light transmitted by the optical train.

The typical results of the checking measurements are given in Table 4.

The accuracy of the adjustment of the quarter wave plate (Q) is pretty good, in fact much better than in the case of analyzer.

Zahradnicek Method

The second method employed for the calibration of the settings of the polarizer and the analyzer has been described by Vasicek.[12] This method was originally developed by Zahradnicek.[13] The half-shade method is usually used in this type of calibration. A Nakamura double-plate is placed just in front of the analyzer and a Ramsden's eye-piece is used in the telescope.

The first orientation measurement is performed in such a way that for two different angles of incidence one greater and one smaller than the Brewster angle ϕ_B of the material (usually a glass plate) situated on the table of the ellipsometer, the position of the polarizer is changed in steps of 10° from 0° to 360° and correspondingly the position of the analyzer for extinction is determined with the help of the half-shade. The results of the measurements are

Table 4

Quarter Wave Plate Calibration

P = 187.65 , A = 348.51						
	Q	Δ_+	Δ_-	Q	Δ_+	Δ_-
1	172.37			82.35		0.020
2	37			37		
3	37			37		
4	37			37		
5	37			37		
6	352.37			262.37		
7	37			37		
8	36		0.010	37		
9	37			37		
10	37			37		

$\bar{Q} = (82.37 \pm 0.00_2)°$ or $Q = (82.37 \pm 0.00)° + n \cdot 90°$ $(n = 0,1,2,3)$

then plotted in a figure and the cross-over point corresponds to the right positions of the polarizer and the analyzer. But a determination like this is usually rather rough and therefore for a more accurate and final determination the following procedure is adopted. For several (at least three) angles of polarizer near its roughly determined position the above method is repeated at several angles of incidence (both smaller and greater than Brewster angle). The results of the measurements are again plotted in a figure and the exact positions of both polarizer and analyzer is determined from this figure.

Since the positions of the polarizer and the analyzer have been determined by the "Brewster angle method," only the second part of this Zahradnicek method was employed for precision calibration. Three different positions of polarizer (187°, 188°, 189°) at six angles of incidence (45°, 50°, 70°, 75°, 80°, 85°) were employed. The results of the measurements are given in Fig. 10. The results of this determination are given together with the results obtained by means of the method described previously in Table 5.

Table 5

Comparison of Polarizer and Analyzer Calibration by the Method Using Brewster Angle and Zahradnicek Method

	Brewster Angle Method	Zahradnicek Method
Polarizer (P)	187.65	187.65
Analyzer (A)	348.51	348.50

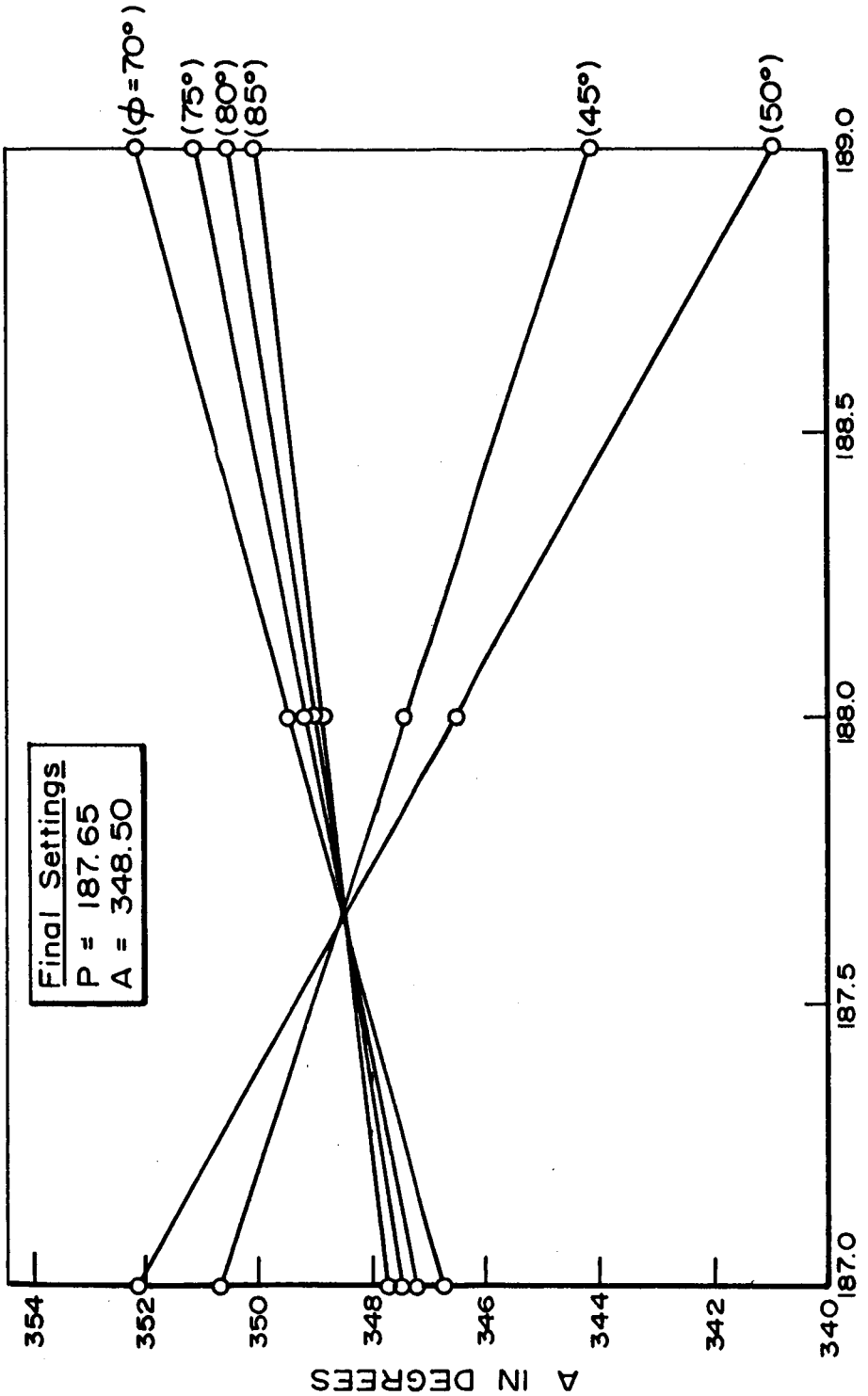

Fig. 10. Zahradnicek curves for the calibration of the polarizer and the analyzer

It is seen that the agreement between the results of the two methods is quite good. The accuracy with which both these settings could be made is thus within $\pm 0.01°$. Since the Zahradnicek method is considered to be more accurate, these values were used as the final settings of the polarizer and analyzer for further measurements.

V. SIMULTANEOUS DETERMINATION OF REFRACTIVE INDEX AND THE THICKNESS OF THE OXIDE FILM ON SILICON

As mentioned in Chapter I our interest is to explore the possibility of a simultaneous determination of the refractive index and the thickness of the film using two fluids as the first medium. From our results in Chapter II, it is seen that the sensitivity relative to film thickness is about the same as in air when we use a liquid like toluene as the first medium. Hence with a slight modification of the existing experimental technique it is possible to determine Δ and ψ with the sample in air and in a liquid, to about the same degree of accuracy. If the refractive indices of the two fluids used as the first medium are n_{01} and n_{02} and the experiments are performed on the same specimen with the same film thickness then we can write

$$\delta_1 = \frac{2\pi d}{\lambda} (n_1^2 - n_{01}^2 \sin^2 \phi_0)^{1/2}$$
$$\delta_2 = \frac{2\pi d}{\lambda} (n_1^2 - n_{02}^2 \sin^2 \phi_0)^{1/2} \qquad (5.1)$$

Here δ_1 and δ_2 are evaluated from the measured values of Δ and ψ using the two fluids as the first medium. From these two equations n_1 and d can be determined independently.

However the evaluation of δ from the measured ellipticity parameters Δ and ψ, requires a knowledge of the refractive index of the film. Thus the above method of determining the refractive index

of the film from measurements in two different fluids, appears to involve a circular argument. However it is possible to employ a self consistency approach to resolve this difficulty. First we assume some reasonable value for the refractive index of the film and evaluate δ_1 and δ_2 from the measured Δ and ψ with the two fluids. From these δ_1 and δ_2 we calculate the refractive index of the film n_1 with the help of equation (5.1). If the assumed value of the refractive index is not correct, the calculated value of the refractive index will come out different from the assumed value. This procedure is repeated for various closely spaced values of the assumed refractive index, till one gets a good agreement between the calculated and the assumed values of the refractive index. In practice the measured values of Δ and ψ will automatically restrict the range of values of the refractive index over which this self consistency procedure is to be carried out. In addition a knowledge of the nature of the film will permit us to work only with such values of refractive index which are physically reasonable. For example in the case of the oxide film on silicon we can reasonably assume that the refractive index will be in the range 1.44 to 1.55. The accuracy in the determination of the refractive index of the film by the self consistency procedure is quite high, as will be seen from the discussion below.

Experimental Procedure and Results

The experimental technique involved in ellipsometry has already been described earlier in the thesis. The only modification

involved in the liquid technique is the provision for a sample holder to hold the specimen in the liquid contained in a suitable cell. The silicon samples, used in the measurements, were cut from a silicon-pulled crystal obtained from Texas Instruments Incorporated. The crystal was oriented in the [111] direction. The resistivity of the silicon crystal was 15-30 ohm cm. When the resistivity is in this range, the crystal cleaves easily in the (111) plane by the Gobeli and Allen technique. This cell was so designed that light enters and leaves the cell normal to the cell windows. The two cell windows were inclined at 40° to each other so that the incident and reflected light rays make an angle of 140° with each other. The sample holder was a goniometric head suitably mounted in the liquid cell. With this arrangement the reflecting surface of the sample could be easily centered and adjusted to coincide with the vertical axis of rotation passing through the center of the table of the ellipsometer. All these adjustments could be done without disturbing the cell and a suitable portion of the sample was used for light incident at an angle of incidence of 70° with the above arrangement.

It must be mentioned here that the proper orientation and centering of the sample is absolutely necessary in this technique as otherwise a large error is introduced in the measured values of the angles of polarizer and analyzer. The results reported here are on silicon samples cleaved parallel to the (111) plane using the well-known technique of Gobeli and Allen.[14] The samples were heated in a clean furnace and due care was taken that no additional dislocation sources or contamination were formed on the surface. This was

achieved by protecting the surface of the sample by not letting the surface touch or be touched by any other object after cleavage. The samples were kept on a platinum foil while being heated. The heated samples were aged in air for a day or two so that the thickness of the SiO_2 film on Si stabilized to a constant value, and would not change during the time involved in measurements.

Independent determinations of Δ and ψ were made by using the method described above both in the case of air and liquid. In the present measurements the liquid used was either toluene or benzene. Both the liquids whenever used were from a freshly opened bottle of analytic reagent type liquid. The refractive indices of toluene and benzene used were experimentally found using an Abbe Refractometer.[15] The Abbe Refractometer used was capable of measuring refractive indices of liquids from 1.3 to 1.7 on a scale which could be read to 0.0001 with an accuracy of 0.0002. The refractometer was maintained at a constant temperature by allowing water from a constant temperature bath to circulate around the liquid sample and the prisms. The values found are 1.4956 and 1.4992 respectively at 23.0°C from an average of ten measurements as shown in Table 6. All the measurements on ellipsometry were made in an air conditioned room where the temperature was also maintained at the above value.

From the measured values of Δ and ψ, the value of δ was evaluated with the help of the computed tables (some of the relevant tables are included in Appendix C). The self consistency procedure described above was applied. Figure 11 shows how the correct value of the refractive index of the film was obtained by this method. In

Table 6

Determination of Index of Refraction of Toluene and Benzene Using Abbe Refractometer

Temperature: 23.0°C		
SNO	Refractive Index of Toluene	Refractive Index of Benzene
1	1.4955	1.4991
2	1.4957	1.4992
3	1.4956	1.4992
4	1.4956	1.4991
5	1.4956	1.4992
6	1.4955	1.4992
7	1.4956	1.4992
8	1.4956	1.4992
9	1.4956	1.4992
10	1.4956	1.4992

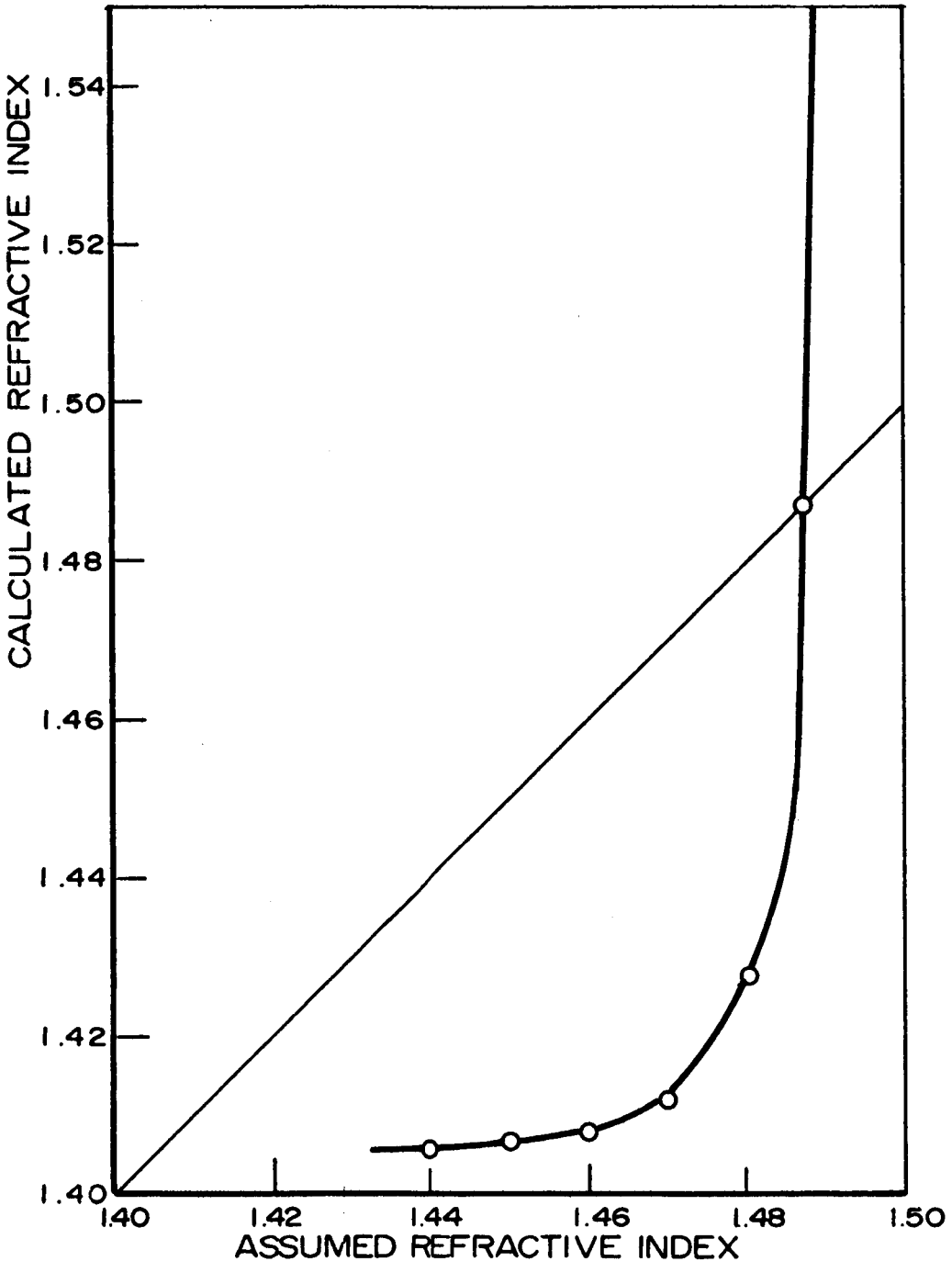

Fig. 11. Plot of the computed values of the refractive index of film against the assumed values, in the self consistency procedure

this figure the computed values of the refractive index of the film are plotted as a function of the assumed values. The intersection of this curve with the straight line at 45° to the axis of the abscissa gives the actual value of the refractive index of the film. If the assumed value of the refractive index is less than this correct value, the calculated value comes out to be lower than the assumed value. On the other hand if the assumed value is more than the correct value, the calculated value comes out to be higher than the assumed value. Very close to the correct value of the refractive index the calculated value varies steeply with the assumed value. Hence the correct value of the refractive index can be fixed very precisely.

An estimate of the error in the refractive index of the film determined by this procedure was made as follows. The measured value of Δ was changed by $\pm 2°$ and the self consistency procedure was applied in the two cases to calculate the corresponding values of the refractive index of the film. It is found that this change of $\pm 2°$ in Δ causes an error of ± 0.004 in the value of the refractive index. For film thickness less than 60 Å, the limit of error in the refractive index is more. In the present series of measurements the value of Δ in the liquid can be determined to $\pm 1°$ and in air to $\pm 0.02°$.

Table 7 gives the values of the refractive index and the film thickness determined by the above method on seven samples of silicon with varying oxide film thicknesses. The samples 2a and 2b as well as 4a and 4b are matched pairs of cleaved surfaces oxidized and

Table 7

Refractive Index of Thin SiO_2 Film

Sample No.	Experimentally Measured Values: In Air Δ(°)	In Air ψ(°)	In Liquid Δ(°)	In Liquid ψ(°)	Liquid Used	Refractive Index of Film	Thickness of Film (Å)
1	115.62	17.84	353.62	1.92	Toluene	1.486 ± 0.004	262
2a	113.92	18.18	353.91	1.91	Toluene	1.487 ± 0.004	273
2b	115.98	17.80	341.92	2.17	Benzene	1.480 ± 0.002	262
3	171.74	11.82	4.86	1.92	Benzene	1.480 ± 0.015	24
4a	153.46	12.60	3.40	1.84	Toluene	1.487 ± 0.005	84
4b	153.74	12.60	358.30	1.93	Benzene	1.479 ± 0.005	84
5	137.68	13.98	351.98	1.98	Benzene	1.480 ± 0.003	147
6*	132.71	14.89	357.13	1.88	Toluene	1.485 ± 0.005	168
7*	154.41	12.74	3.18	1.78	Toluene	1.486 ± 0.003	81

*Measurements of Dr. F. Lukes shown here for comparison

handled under similar conditions. The table also gives the liquid in which the measurements were carried out.

The following conclusions can be reached. All the seven different specimens give consistent values for the refractive index of the film. The average value of the refractive index thus found is 1.484 ± 0.004. Measurements on matched pair of specimens with two different liquids give the same value for the film thickness within the limits of accuracy.

In all the previous investigations[5,7] on the kinetics of oxidation of silicon, the refractive index of the oxide film was taken to be 1.460, that of vitreous silica. The ordered forms of SiO_2 like cristobalite, α-quartz, etc. have considerably higher value than 1.460. The present direct determination of the refractive index of the oxide film gives a value 1.484 which definitely indicates that the oxide film has a high degree of order at such small film thicknesses (< 300 Å). In fact this value is close to the refractive index of cristobalite. It is not known whether it could be concluded from these measurements that these oxide films have the cristobalite structure. It would be interesting if one could obtain a more direct evidence about the structure of these oxide films, say by the Low Energy Electron Diffraction technique.

VI. SUMMARY AND CONCLUSIONS

In ellipsometry, the interesting case of light incident from a dense medium like liquid on to a film over an absorbing substrate has been studied theoretically for the two cases: (i) when the angle of incidence ϕ_0 is less than the critical angle ϕ_c and (ii) when $\phi_0 > \phi_c$. Detailed calculations have indicated that the sensitivity with which the thickness of the film with an assumed refractive index can be measured is nearly the same whatever be the first medium for the case when $\phi_0 < \phi_c$. When $\phi_0 > \phi_c$, the sensitivity is very poor.

It has been further shown that by combining the two sets of measurements on the ellipticity parameters with air and a liquid as the first medium, it is possible to evaluate the thickness and the refractive index of the film independently by a self consistency procedure. Measurements on oxide films on a substrate of silicon by ellipsometer with the samples immersed in air or benzene or toluene indicate that the value of the refractive index of the thin films in the range 80-300 Å is 1.484 ± 0.004 for λ5461 Å and not 1.460 as has been assumed by previous workers. Hence, it is necessary to revise the earlier conclusions of Archer[7] regarding the oxidation kinetics of silicon, since they were based on the assumption that the refractive index of the silicon dioxide is 1.460. Finally, it should be noted that this is the first time the

refractive index and the thickness of the very thin film ($\approx$80 to 200 Å) in an absorbing substrate has been independently determined.

Suggestions for Further Research

With the instrumentation developed and described earlier in the thesis, it is now possible to study the growth of SiO_2 film on Si starting from the crystal cleavage time to the time when the film growth is stabilized. These measurements require an ultra high vacuum system with a facility to control partial pressure of oxygen and also a facility to cleave the crystal in vacuum. All these systems have already been designed and fabricated by the author. The crystals can now be cleaved in vacuum by the Gobeli and Allen[14] technique; and the partial pressure of oxygen can be controlled by two methods: (i) by introducing a controlled oxygen lead in the system and (ii) by a buffering system of FeO-Fe_2O_3 introduced in the vacuum line with an arrangement to control the temperature of this mixture precisely. These measurements should reveal the mechanism and kinetics of oxidation of silicon completely.

It will also be interesting to study the structure of these thin SiO_2 films (less than 200 Å). Low energy electron diffraction experiments performed on these films may give a clue to the structure.

BIBLIOGRAPHY

1. P. Drude, Ann. Physik., 272, 532 (1889); ibid., 272, 865 (1889); ibid., 275, 481 (1890)

2. R. J. Archer, Jour. Electrochem. Soc., 104, 619 (1957)

3. A. N. Saxena, Jour. Opt. Soc. Amer., 55, 1061 (1965)

4. D. K. Burge and H. E. Bennett, J. Opt. Soc. Am., 54, 1428 (1964)

5. R. J. Archer and G. W. Gobeli, J. Phys. Chem. Solids, 26, 343 (1965)

6. A. Vasicek, "Optics of Thin Films," North Holland Publishing Company, Amsterdam, 1960, p. 365

7. R. J. Archer, Jour. Opt. Soc. Amer., 52, 960 (1962)

8. E. Passaglia and R. R. Stromberg, Jour. Physics and Chemistry, 68A, 601 (1964)

9. "Ellipsometry in the Measurement of Surfaces and Thin Films," Ed., E. Passaglia, R. R. Stromberg and J. Kruger, Nat. Bur. Stds., Misc. Publ. No. 256 (1964)

10. O. S. Heavens, "Optical Properties of Thin Solid Films," Butterworths, London (1955)

11. R. J. Archer, "Ellipsometry in the Measurement of Surfaces and Thin Films," Ed., E. Passaglia, R. R. Stromberg and J. Kruger, Nat. Bur. Stds., Misc. Publ. No. 256 (1964), p. 255

12. A. Vasicek, Mereri a ytrareni tenkych vrstev v optice (in Czech), Publishing House of the Czechoslovakian Academy of Sciences, Prague, 1957, p. 26

13. J. Zahradnicek, Casopis pro pestovani matematiky a fyziky, 54, 354 (1925)

14. G. W. Gobeli and F. G. Allen, Jour. Phys. Chem. Solids, 14, 23 (1960)

15. B. L. Worsnop and H. T. Flint, "Advanced Practical Physics," Mathuen and Co., Ltd., London, p. 295

16. S. R. Sashital (Ph.D. Thesis, 1967, The Pennsylvania State University)

17. A. K. N, Reddy and J. O'M. Bokris, "Ellipsometry in Electrochemical Studies," Ed., E. Passaglia, R. R. Stromberg and J. Kruger, Nat. Bur. Stds., Misc. Publ. No. 256 (1964), p. 229

APPENDIX A

A DAFT Program for the Interpretation of Ellipsometric Measurements for $\phi_0 < \phi_c$

```
BEGIN MULTIPLE DECK COMPILE
BEGIN DAFT SOURCE DECK
            RAD(A)=A*3.1415927/180.
            DEG(A)=(A*180.)/3.1415927
            DIMENSION RNX(21),DEL(2,216),DELTA(2,216),PSI(2,216),XP(216),
           1YP(216)
            READ 100 ,N,A,RNX2,RK2
C  REFRACTIVE INDEX OF SILICON= RNX2-I*(RK2)
C  REFRACTIVE INDEX OF SILICON OXIDE =RNX1
      100   FORMAT(T7,I4,T15,F6.2,T25,F6.3,T35,F4.3)
            A=RAD(A)
            SINA=SIN(A)
            COSA=COS(A)
            RNXA=1.496
            ALPHA1=(RNX2**2)-(RK2**2)-(SINA**2)
            ALPHA2=2.*RNX2*RK2
            RNO=SQRT(ALPHA1**2+ALPHA**2)
            APHI=-ATAN(ALPHA2/ALPHA1)
            R1NO=SQRT( NX2**2+RK2**2)
            APHI1=-ATAN(RK2/RNX2)
            R2NO=SQRT(RNO)/R1NO
            APHI2=APHI/2.0 - APHI1
            ALPHA3=R2NO*COS(APHI2)
            ALPHA4=R2NO*SIN(APHI2)
            DEL(1,1)=0.
            DEL(2,1)=0.
            DO 200 J=1,40
            DEL(1,J+1)=DEL(1,J)+0.01
      200   DEL(2,J+1)=RAD(2.0*DEL(1,J+1))
            DO 201 JJ=1,16
            DEL(1,JJ+41)=DEL(1,JJ+40)+0.10
      201   DEL(2,JJ+41)=RAD(2.0*DEL(1,JJ+41))
            DO 202 JJJ=1,20
            DEL(1,JJJ+57)=DEL(1,JJJ+56)+0.20
      202   DEL(2,JJJ+57)=RAD(2.0*DEL(1,JJJ+57))
            DO 203 K=1,4
            DEL(1,K+77)=DEL(1,K+76)+1.0
      203   DEL(2,K+77)=RAD(2.0*DEL(1,K+77))
            DEL(1,82)=12.0
            DEL(2,82)=RAD(2.0*DEL(1,82))
            DO 204 KK=1,8
            DEL(1,KK+82)=DEL(1,KK+81)+0.50
      204   DEL(2,KK+82)=RAD(2.0*DEL(1,KK+82))
            DO 205 KKK=1,36
            DEL(1,KKK+90)=DEL(1,KKK+89)+4.0
      205   DEL(2,KKK+90)=RAD(2.0*DEL(1,KKK+90))
            DEL(1,127)=164.0
            DEL(2,127)=RAD(2.0*DEL(1,127))
            DO 206 L=1,8
            DEL(1,L+127)=DEL(1,L+126)+0.50
      206   DEL(2,L+127)=RAD(2.0*DEL(1,127))
            DE (1,136)=170.0
            DEL(2,136)=RAD(2.0*DEL(1,136))
            DO 207 LL=1,3
            DEL(1,LL+136)=DEL(1,LL+135)+1.0
      207   DEL(2,LL+136)=RAD(2.0*DEL(1,LL+136))
            DEL(1,140)=174.0
            DEL(2,140)=RAD(2.0*DEL(1,140))
            DO 208 LLL=1,19
            DEL(1,LLL+140)=DEL(1,LLL+139)+0.20
```

```
208   DEL(2,LLL+140)=RAD(2.0*DEL(1,LLL+140))
      DEL(1,160)=178.0
      DEL(2,160)=RAD(2.0*DEL(1,160))
      DO 209 M=1,15
      DEL(1,M+160)=DEL(1,M+159)+0.10
209   DEL(2,M+160)=RAD(2.0*DEL(1,M+160))
      DEL(1,176)=179.60
      DEL(2,176)=RAD(2.0*DEL(1,176))
      DO 210 MM=1,39
      DEL(1,MM+176)=DEL(1,MM+175)+0.01
210   DEL(2,MM+176)=RAD(2.0*DEL(1,MM+176))
      DEL(1,216)=180.0
      DEL(2,216)=RAD(2.0*DEL(1,216))
      READ 101, (RNX(J),J=1,N)
101   FORMAT(8F10.3)
      DO 1000 I=1,N
      RNX1=RNX(I)
      COSB=COS(ASIN(SINA*RNXA/RNX1))
      RD=RNX1*ALPHA3-RNX2*COSB
      RE=RNX1*ALPHA4+RK2*COSB
      RF=RNX1*ALPHA3+RNX2*COSB
      RG=RNX1*ALPHA4-RK2*COSB
      RI=RNX1*COSB-RNX2*ALPHA3-RK2*ALPHA4
      RJ=RK2*ALPHA3-RNX2*ALPHA4
      RK=RNX1*COSB+RNX2*ALPHA3+RK2*ALPHA4
      RN=RNX2*ALPHA4-RK2*ALPHA3
      SCH1=RNXA*COSB
      SCH2=RNXA*COSA
      CALL POLMOR(RD,RE,RF,RG,SCH1,COSA,RL,RO,RP,RNX1)
      CALL POLMOR(RI,RJ,RK,RN,SCH2,COSB,RM,RQ,RR,RNX1)
      DO 300 J=1,216
      CS2D=COS(DEL(2,J))
      SN2D=SIN(DEL(2,J))
      CALL STUVWX(RL,RO,RP,CS2D,SN2D,W,X)
      CALL STUVWX(RM,RO,RR,CS2D,SN2D,W1,X1)
      DENR=W1**2+X1**2
      Y=(W*W1+X*X1)/DENR
      Z=(X*W1-W*X1)/DENR
      DELTA(1,J)=ATAN(Z/Y)
      PSI(1,J)=ATAN(Y/COS(DELTA(1,J)))
      DELTA(2,J)=DEG(DELTA(1,J))
      PSI(2,J)=DEG(PSI(1,J))
      IF(PSI(2,J)) 500,401,401
500   PSI(2,J)=-PSI(2,J)
      DELTA(2,J)=DELTA(2,J)+360.
      IF(DELTA(2,J)-360.0)402,402,700
700   DELTA(2,J)=DELTA(2,J)-360.
402   GO TO 300
401   DELTA(2,J)=DELTA(2,J)+180.
300   CONTINUE
      DO 600 J=1,216
      YP(J)=DELTA(2,J)/18.0
600   XP(J)=PSI(2,J)/10.0
      PRINT 110,RNX(I)
110   FORMAT('1'133,'INDEX OF REFRACTION ='F6.3/'0'3('SMALL'28X)/
     11X3('DELTA'6X'DELTA'7X'PSI'7X)/)
      DO 501,J=1,72
501   PRINT 120,DEL(1,J),DELTA(2,J),PSI(2,J),DEL(1,J+72),DELTA(2,J+72),
     1PSI(2,J+72),DEL(1,J+144),DELTA(2,J+144),PSI(2,J+144)
120   FORMAT(1X3(F6.2,4X,F7.3,4X,F7.3,6X))
```

```
            IF(I-1)602,601,602
      601   CALL TAPEMOUNT(14,10HSILICON 01,0)
            CALL TAPEMOD(14,0,0)
            CALL TAPECHECK
            CALL AXIS(0.0,0.0,8HPSI-AXIS,-8,9.0,0.0,0.0,10.0)
            CALL AXIS(0.0,0.0,10HDELTA-AXIS,10,20.0,90.0,0.0,18.0)
            CALL PLOT(XP(1),YP(1),3)
      602   DO 603 J=1,108
      603   CALL PLOT(XP(J),YP(J),2)
            XN=XP(108)+0.10
            YN=YP(108)+0.10
            CALL NUMBER(XN,YN,0.1,RNX(I),0.0,3)
            CALL PLOT(XP(108),YP(108),3)
            DO 604 J=108,216
      604   CALL PLOT(XP(J),YP(J),2)
            DO 605 J=1,216,20
      605   CALL SPECSYMBOL(XP(J),YP(J),0.125,7,0.0,+1)
            CALL PLOT(XP(211),YP(211),3)
      1000  CONTINUE
            CALL PLOT(0.0,0.0,-3)
            ENDFILE 14
            CALL TAPEDONE(14)
            STOP
END DAFT SOURCE DECK
BEGIN DAFT SOURCE DECK
            SUBROUTINE POLMOR(RO,RE,RF,RG,X1,X2,RL,RO,RP,RNX1)
            REG=(RE**2+RG**2)
            RL=(X1-RNX1*X2)/(X1+RNX1*X2)
            RO=(RO*RF+RE*RG)/REG
            RP=(RE*RF-RO*RG)/REG
            RETURN
END DAFT SOURCE DECK
BEGIN DAFT SOURCE DECK
            SUBROUTINE STUVWX(RL,RO,RP,CS2O,SN2O,W,X)
            RS=RL+RO*CS2O+RP*S 2O
            RT=RP*CS2O-RO*SN2O
            RO=1.+RL*RO*CS2O+RL*RP*SN2O
            RV=RL*RP*CS2O-RL*RO*SN2O
            ROV=RO**2+RV**2
            W=(RS*RO+RT*RV)/ROV
            X=(RT*RO-RS*RV)/ROV
            RETURN
END DAFT SOURCE DECK
END MULTIPLE DECK COMPILE
```

APPENDIX B

A DAFT Program for the Interpretation of Ellipsometric Measurements for $\phi_0 > \phi_c$

```
BEGIN DAFT SOURCE DECK
      RAD(A)=A*3.1415927/180.
      DEG(A)=(A*180.)/3.1415927
      DIMENSION RNX(1),X1(2,181),DELTA(2,181),PSI(2,181)
      READ 100,N,PHI0,RNX0,RNX2,RK2
  100 FORMAT(T10,I2,T20,F6.2,T30,F8.6,T40,F8.3,T50,F8.3)
      PHI0 = RAD(PHI0)
      SINPHI0=SIN(PHI0)
      COSPHI0=COS(PHI0)
      A1=RNX0*COSPHI0
      A2=(RNX0**2)*(SINPHI0**2)
      A3=RNX2**2-RK2**2-A2
      A4=-2.*RNX2*RK2
      A5=SQRT(A3**2+A4**2)
      THETA1=ATAN(A4/A3)
      A62=SQRT(A5)
      A61=A62*(COS(THETA1/2.))
      A6=A1-A61
      A7=A1+A61
      A8=A62*(SIN(THETA1/2.))
      A9=A7**2+A8**2
      A10 A6*A7-A8**2
      A11=A7*A8+A6*A8
      A12=A10/A9
      A13=-A11/A9
      A14=SQRT(A12**2+A13**2)
      THETA2=ATAN(A13/A12)
      B1=RNX2*COSPHI0
      B2=RNX0/(RNX2**2+RK2**2)
      B3=A3*RNX2-RK2*A4
      B4=RK2*COSPHI0
      B5=A4*RNX2+RK2*A3
      B6=B1-B2*B3
      B7=B4+B2*B5
      B8=B1+B2*B3
      B9=B4-B2*B5
      B10=B8**2+B9**2
      B13=(B6*B8+B7*B9)/B10
      B14=(B6*B9-B7*B8)/B10
      B15=SQRT(B13**2+B14**2)
      THETA3=ATAN(B14/B13)
      X1(1,1)=0.
      X1(2,1)=0.
      DO 200 J=1,180
      X1(1,J+1)=X1(1,J)+2.0
  200 X1(2,J+1)=RAD(2.0*X1(1,J+1))
      READ 101, (RNX(J),J=1,N)
  101 FORMAT(8F10.3)
      DO 5000 I=1,N
      RNX1=RNX(I)
      A=SQRT(A2-RNX1**2)/A1
      DELS1=2.*ATAN(A)
      DELP1=2.*ATAN((RNX0**2/RNX1**2)*A)
      DELS2=2.*DELS1
      DELP2=2.*DELP1
      B=COS(DELP1)
      C=SIN(DELP1)
      D=COS(DELS1)
      E=SIN(DELS1)
      R=COS(DELP2)
```

```
      S=SIN(DELP2)
      T=COS(DELS2)
      Q=SIN(DELS2)
      C1=B15*B13*B
      C2=B15*B14*C
      C3=B15*B13*C
      C4=B15*B14*B
      C5=1.0-(C1-C2)
      C6=C3+C4
      C7=1.0-(C1+C2)
      C8=C4-C3
      D1=A14*A12*D
      D2=A14*A13*E
      D3=A14*A12*E
      D4=A14*A13*D
      D5=1.0-(D1-D2)
      D6=D3+D4
      D7=1.0-(D1+D2)
      D8=D4-D3
      DO 300 J=1,181
      RNUMBER=1./EXP(X1(2,J))
      C9=C5-C7/RNUMBER
      C10= C8/RNUMBER-C6
      C11=C5-(R*C7+S*C8)/RNUMBER
      C12= -(C6+(S*C7)/RNUMBER-(R*C8)/RNUMBER)
      C13=B*C9-C*C10
      C14=C*C9+B*C10
      C15=(C13*C11+C14*C12)/(C11**2+C12**2)
      C16=(C14*C11-C12*C13)/(C11**2+C12**2)
      D9=D5-D7/RNUMBER
      D10=D8/RNUMBER-D6
      D11=D5-(T*D7+Q*D8)/RNUMBER
      D12= -(D6+(Q*D7)/RNUMBER-(T*D8)/RNUMBER)
      D13=D*D9-E*D10
      D14=E*D9+D*D10
      D15=(D13*D11+D14*D12)/(D11**2+D12**2)
      D16=(D14*D11-D12*D13)/(D11**2+D12**2)
      D1516=D15**2+D16**2
      U=(C15*D15+C16*D16)/D1516
      V=(C16*D15-C15*D16)/D1516
      DELTA(1,J)=ATAN(V/U)
      PSI(1,J)=ATAN(U/COS(DELTA(1,J)))
      DELTA(2,J)=DEG(DELTA(1,J))
      PSI(2,J)=DEG(PSI(1,J))
      IF(PSI(2,J)) 500,401,401
  500 PSI(2,J)=-PSI(2,J)
      DELTA(2,J)=DELTA(2,J)+360.
      IF(DELTA(2,J)-360.0)402,402,700
  700 DELTA(2,J)=DELTA(2,J)-360.
  402 GO TO 300
  401 DELTA(2,J)=DELTA(2,J)+180.
  300 CONTINUE
      PRINT 110,RNX(I)
  110 FORMAT('1'T33,'INDEX OF REFRACTION = 'F6.3/'0'3('SMALL'28X)/
     11X3('DELTA'6X'DELTA'7X'PSI'7X)/)
      DO 501 J=1,60
  501 PRINT 120,X1(1,J),DELTA(2,J),PSI(2,J),X1(1,J+60),DELTA(2,J+60),
     1PSI(2,J+60),X1(1,J+120),DELTA(2,J+120),PSI(2,J+120)
  120 FORMAT(1X3(F5.1,4X,F7.3,4X,F7.3,6X))
 5000 PRINT 130,X1(1,181),DELTA(2,181),PSI(2,181)
  130 FORMAT(168,F5.1,4X,F7.3,4X,F7.3)
      STOP
END DAFT SOURCE DECK
```

APPENDIX C

A Sample of Computed Tables

$n_0 = 1.0$, $n_1 = 1.460$, $\lambda = 5461$ Å

SMALL DELTA	DELTA	PSI	SMALL DELTA	DELTA	PSI	SMALL DELTA	DELTA	PSI
0.00	179.038	11.763	5.20	157.814	12.353	175.00	199.623	12.227
0.01	178.996	11.763	5.40	157.045	12.396	175.20	198.835	12.190
0.02	178.954	11.763	5.60	156.282	12.441	175.40	198.043	12.154
0.03	178.912	11.763	5.80	155.523	12.486	175.60	197.248	12.120
0.04	178.870	11.764	6.00	154.770	12.534	175.80	196.448	12.087
0.05	178.828	11.764	7.00	151.080	12.788	176.00	195.644	12.056
0.06	178.786	11.764	8.00	147.528	13.073	176.20	194.837	12.026
0.07	178.744	11.764	9.00	144.117	13.385	176.40	194.026	11.998
0.08	178.702	11.764	10.00	140.850	13.722	176.60	193.212	11.971
0.09	178.659	11.764	12.00	134.748	14.460	176.80	192.395	11.946
0.10	178.617	11.764	12.50	133.309	14.656	177.00	191.574	11.922
0.11	178.575	11.764	13.00	131.905	14.857	177.20	190.751	11.900
0.12	178.533	11.765	13.50	130.535	15.061	177.40	189.925	11.880
0.13	178.491	11.765	14.00	129.197	15.269	177.60	189.097	11.861
0.14	178.449	11.765	14.50	127.891	15.480	177.80	188.266	11.844
0.15	178.407	11.765	15.00	126.617	15.695	178.00	187.434	11.828
0.16	178.365	11.765	15.50	125.373	15.912	178.10	187.017	11.821
0.17	178.323	11.765	16.00	124.159	16.132	178.20	186.599	11.814
0.18	178.281	11.765	20.00	115.428	17.965	178.30	186.181	11.808
0.19	178.239	11.766	24.00	108.188	19.874	178.40	185.763	11.802
0.20	178.197	11.766	28.00	102.137	21.807	178.50	185.344	11.797
0.21	178.154	11.766	32.00	97.054	23.739	178.60	184.925	11.791
0.22	178.112	11.766	36.00	92.786	25.664	178.70	184.506	11.787
0.23	178.070	11.766	40.00	89.233	27.591	178.80	184.087	11.782
0.24	178.028	11.767	44.00	86.333	29.546	178.90	183.667	11.779
0.25	177.986	11.767	48.00	84.052	31.570	179.00	183.247	11.775
0.26	177.944	11.767	52.00	82.380	33.721	179.10	182.826	11.772
0.27	177.902	11.767	56.00	81.325	36.081	179.20	182.406	11.769
0.28	177.860	11.767	60.00	80.912	38.762	179.30	181.985	11.767
0.29	177.818	11.768	64.00	81.183	41.916	179.40	181.564	11.765
0.30	177.776	11.768	68.00	82.199	45.747	179.50	181.143	11.764
0.31	177.734	11.768	72.00	84.059	50.520	179.60	180.722	11.763
0.32	177.692	11.768	76.00	86.954	56.551	179.61	180.680	11.763
0.33	177.650	11.768	80.00	91.389	64.139	179.62	180.638	11.763
0.34	177.607	11.769	84.00	99.280	73.352	179.63	180.596	11.763
0.35	177.565	11.769	88.00	125.555	83.319	179.64	180.554	11.763
0.36	177.523	11.769	92.00	237.920	82.725	179.65	180.512	11.763
0.37	177.481	11.769	96.00	261.243	72.711	179.66	180.470	11.763
0.38	177.439	11.770	100.00	268.765	63.590	179.67	180.428	11.762
0.39	177.397	11.770	104.00	273.067	56.104	179.68	180.386	11.762
0.40	177.355	11.770	108.00	275.883	50.158	179.69	180.344	11.762
0.50	176.935	11.773	112.00	277.680	45.450	179.70	180.301	11.762
0.60	176.514	11.776	116.00	278.639	41.666	179.71	180.259	11.762
0.70	176.094	11.780	120.00	278.858	38.543	179.72	180.217	11.762
0.80	175.675	11.784	124.00	278.394	35.882	179.73	180.175	11.762
0.90	175.255	11.788	128.00	277.289	33.533	179.74	180.133	11.762
1.00	174.836	11.793	132.00	275.566	31.386	179.75	180.091	11.762
1.10	174.417	11.798	136.00	273.232	29.363	179.76	180.049	11.762
1.20	173.998	11.804	140.00	270.274	27.406	179.77	180.007	11.762
1.30	173.580	11.810	144.00	266.656	25.474	179.78	179.965	11.762
1.40	173.162	11.816	148.00	262.313	23.545	179.79	179.922	11.762
1.50	172.745	11.823	152.00	257.140	21.609	179.80	179.880	11.762
1.60	172.328	11.830	156.00	250.977	19.673	179.81	179.838	11.762
1.70	171.912	11.838	160.00	243.596	17.767	179.82	179.796	11.762
1.80	171.496	11.846	164.00	234.686	15.945	179.83	179.754	11.762
1.90	171.080	11.855	164.50	234.686	15.945	179.84	179.712	11.762
2.00	170.666	11.864	165.00	234.686	15.945	179.85	179.670	11.762
2.20	169.838	11.883	165.50	234.686	15.945	179.86	179.628	11.762
2.40	169.012	11.903	166.00	234.686	15.945	179.87	179.586	11.762
2.60	168.190	11.926	166.50	234.686	15.945	179.88	179.544	11.762
2.80	167.370	11.949	167.00	234.686	15.945	179.89	179.501	11.762
3.00	166.553	11.975	167.50	234.686	15.945	179.90	179.459	11.762
3.20	165.739	12.002	168.00	234.686	15.945	179.91	179.417	11.763
3.40	164.929	12.030	170.00	217.651	13.575	179.92	179.375	11.763
3.60	164.122	12.060	171.00	214.322	13.248	179.93	179.333	11.763
3.80	163.319	12.092	172.00	210.850	12.947	179.94	179.291	11.763
4.00	162.520	12.125	173.00	207.237	12.675	179.95	179.249	11.763
4.20	161.725	12.159	174.00	203.492	12.434	179.96	179.207	11.763
4.40	160.934	12.195	174.20	202.727	12.390	179.97	179.165	11.763
4.60	160.147	12.233	174.40	201.958	12.347	179.98	179.123	11.763
4.80	159.365	12.271	174.60	201.184	12.306	179.99	179.080	11.763
5.00	158.587	12.312	174.80	200.406	12.266	180.00	179.038	11.763

$n_0 = 1.0$, $n_1 = 1.484$, $\lambda = 5461$ Å

SMALL DELTA	DELTA	PSI	SMALL DELTA	DELTA	PSI	SMALL DELTA	DELTA	PSI
0.00	179.038	11.763	5.20	157.894	12.342	175.00	199.541	12.218
0.01	178.996	11.763	5.40	157.128	12.385	175.20	198.756	12.181
0.02	178.955	11.763	5.60	156.366	12.428	175.40	197.967	12.146
0.03	178.913	11.763	5.80	155.609	12.473	175.60	197.173	12.113
0.04	178.871	11.764	6.00	154.857	12.519	175.80	196.376	12.080
0.05	178.829	11.764	7.00	151.173	12.769	176.00	195.575	12.050
0.06	178.787	11.764	8.00	147.622	13.049	176.20	194.771	12.021
0.07	178.745	11.764	9.00	144.210	13.356	176.40	193.963	11.993
0.08	178.703	11.764	10.00	140.940	13.687	176.60	193.152	11.967
0.09	178.661	11.764	12.00	134.821	14.414	176.80	192.337	11.942
0.10	178.619	11.764	12.50	133.377	14.607	177.00	191.520	11.919
0.11	178.577	11.764	13.00	131.967	14.805	177.20	190.700	11.897
0.12	178.535	11.765	13.50	130.590	15.006	177.40	189.878	11.877
0.13	178.494	11.765	14.00	129.245	15.211	177.60	189.053	11.859
0.14	178.452	11.765	14.50	127.932	15.419	177.80	188.226	11.842
0.15	178.410	11.765	15.00	126.649	15.631	178.00	187.397	11.827
0.16	178.368	11.765	15.50	125.397	15.845	178.10	186.981	11.820
0.17	178.326	11.765	16.00	124.174	16.062	178.20	186.566	11.813
0.18	178.284	11.765	20.00	115.364	17.872	178.30	186.150	11.807
0.19	178.242	11.766	24.00	108.029	19.761	178.40	185.733	11.801
0.20	178.200	11.766	28.00	101.874	21.677	178.50	185.316	11.796
0.21	178.158	11.766	32.00	96.678	23.595	178.60	184.899	11.791
0.22	178.117	11.766	36.00	92.287	25.508	178.70	184.482	11.786
0.23	178.075	11.766	40.00	88.600	27.425	178.80	184.064	11.782
0.24	178.033	11.766	44.00	85.552	29.373	178.90	183.646	11.778
0.25	177.991	11.767	48.00	83.104	31.392	179.00	183.228	11.775
0.26	177.949	11.767	52.00	81.239	33.541	179.10	182.809	11.772
0.27	177.907	11.767	56.00	79.958	35.900	179.20	182.391	11.769
0.28	177.865	11.767	60.00	79.271	38.584	179.30	181.972	11.767
0.29	177.823	11.767	64.00	79.197	41.745	179.40	181.553	11.765
0.30	177.781	11.768	68.00	79.760	45.591	179.50	181.134	11.764
0.31	177.740	11.768	72.00	80.986	50.394	179.60	180.715	11.763
0.32	177.698	11.768	76.00	82.910	56.485	179.61	180.673	11.763
0.33	177.656	11.768	80.00	85.635	64.187	179.62	180.631	11.763
0.34	177.614	11.769	84.00	89.658	73.647	179.63	180.589	11.763
0.35	177.572	11.769	88.00	100.425	84.511	179.64	180.547	11.763
0.36	177.530	11.769	92.00	261.016	83.765	179.65	180.505	11.763
0.37	177.488	11.769	96.00	270.489	72.961	179.66	180.463	11.763
0.38	177.446	11.769	100.00	274.381	63.611	179.67	180.421	11.762
0.39	177.405	11.770	104.00	277.044	56.019	179.68	180.379	11.762
0.40	177.363	11.770	108.00	278.916	50.019	179.69	180.338	11.762
0.50	176.944	11.773	112.00	280.091	45.284	179.70	180.296	11.762
0.60	176.526	11.776	116.00	280.606	41.487	179.71	180.254	11.762
0.70	176.108	11.779	120.00	280.484	38.359	179.72	180.212	11.762
0.80	175.690	11.783	124.00	279.749	35.697	179.73	180.170	11.762
0.90	175.272	11.788	128.00	278.419	33.349	179.74	180.128	11.762
1.00	174.855	11.792	132.00	276.505	31.206	179.75	180.086	11.762
1.10	174.438	11.797	136.00	274.004	29.189	179.76	180.044	11.762
1.20	174.021	11.803	140.00	270.897	27.239	179.77	180.002	11.762
1.30	173.605	11.809	144.00	267.146	25.317	179.78	179.960	11.762
1.40	173.189	11.815	148.00	262.681	23.400	179.79	179.918	11.762
1.50	172.773	11.822	152.00	257.394	21.478	179.80	179.877	11.762
1.60	172.358	11.829	156.00	251.126	19.561	179.81	179.835	11.762
1.70	171.943	11.837	160.00	243.651	17.675	179.82	179.793	11.762
1.80	171.529	11.845	164.00	234.661	15.876	179.83	179.751	11.762
1.90	171.116	11.853	164.50	234.661	15.876	179.84	179.709	11.762
2.00	170.702	11.862	165.00	234.661	15.876	179.85	179.667	11.762
2.20	169.878	11.881	165.50	234.661	15.876	179.86	179.625	11.762
2.40	169.056	11.901	166.00	234.661	15.876	179.87	179.583	11.762
2.60	168.236	11.923	166.50	234.661	15.876	179.88	179.541	11.762
2.80	167.420	11.946	167.00	234.661	15.876	179.89	179.499	11.762
3.00	166.606	11.971	167.50	234.661	15.876	179.90	179.457	11.762
3.20	165.795	11.997	168.00	234.661	15.876	179.91	179.416	11.763
3.40	164.988	12.025	170.00	217.555	13.541	179.92	179.374	11.763
3.60	164.184	12.055	171.00	214.223	13.220	179.93	179.332	11.763
3.80	163.384	12.086	172.00	210.750	12.925	179.94	179.290	11.763
4.00	162.587	12.118	173.00	207.141	12.658	179.95	179.248	11.763
4.20	161.795	12.152	174.00	203.401	12.421	179.96	179.206	11.763
4.40	161.006	12.187	174.20	202.638	12.378	179.97	179.164	11.763
4.60	160.221	12.224	174.40	201.871	12.336	179.98	179.122	11.763
4.80	159.441	12.262	174.60	201.099	12.295	179.99	179.080	11.763
5.00	158.666	12.301	174.80	200.322	12.256	180.00	179.038	11.763

$n_0 = 1.4956$, $n_1 = 1.460$, $\lambda = 5461$ Å

SMALL DELTA	DELTA	PSI	SMALL DELTA	DELTA	PSI	SMALL DELTA	DELTA	PSI
0.00	7.686	1.838	5.20	332.045	2.273	175.00	36.840	2.514
0.01	7.607	1.838	5.40	331.144	2.310	175.20	36.128	2.473
0.02	7.528	1.837	5.60	330.281	2.347	175.40	35.381	2.433
0.03	7.449	1.837	5.80	329.455	2.385	175.60	34.599	2.393
0.04	7.370	1.837	6.00	328.666	2.424	175.80	33.781	2.355
0.05	7.291	1.836	7.00	325.230	2.631	176.00	32.926	2.317
0.06	7.212	1.836	8.00	322.546	2.853	176.20	32.033	2.281
0.07	7.133	1.836	9.00	320.487	3.087	176.40	31.100	2.245
0.08	7.054	1.835	10.00	318.941	3.329	176.60	30.128	2.211
0.09	6.974	1.835	12.00	317.029	3.830	176.80	29.116	2.177
0.10	6.895	1.835	12.50	316.744	3.958	177.00	28.062	2.145
0.11	6.816	1.834	13.00	316.523	4.086	177.20	26.968	2.114
0.12	6.737	1.834	13.50	316.359	4.214	177.40	25.832	2.084
0.13	6.657	1.834	14.00	316.247	4.343	177.60	24.655	2.055
0.14	6.578	1.833	14.50	316.182	4.472	177.80	23.436	2.028
0.15	6.499	1.833	15.00	316.160	4.602	178.00	22.177	2.003
0.16	6.419	1.833	15.50	316.177	4.731	178.10	21.533	1.990
0.17	6.340	1.833	16.00	316.230	4.860	178.20	20.879	1.978
0.18	6.260	1.832	20.00	317.610	5.885	178.30	20.215	1.967
0.19	6.181	1.832	24.00	320.034	6.879	178.40	19.542	1.956
0.20	6.101	1.832	28.00	322.948	7.827	178.50	18.859	1.945
0.21	6.022	1.832	32.00	326.060	8.721	178.60	18.167	1.935
0.22	5.942	1.831	36.00	329.206	9.558	178.70	17.467	1.925
0.23	5.863	1.831	40.00	332.291	10.335	178.80	16.757	1.916
0.24	5.783	1.831	44.00	335.265	11.051	178.90	16.039	1.907
0.25	5.703	1.831	48.00	338.102	11.706	179.00	15.313	1.898
0.26	5.624	1.830	52.00	340.792	12.299	179.10	14.580	1.890
0.27	5.544	1.830	56.00	343.336	12.833	179.20	13.839	1.882
0.28	5.464	1.830	60.00	345.741	13.306	179.30	13.090	1.875
0.29	5.385	1.830	64.00	348.019	13.720	179.40	12.335	1.868
0.30	5.305	1.829	68.00	350.185	14.076	179.50	11.574	1.862
0.31	5.225	1.829	72.00	352.254	14.373	179.60	10.807	1.856
0.32	5.145	1.829	76.00	354.243	14.613	179.61	10.729	1.856
0.33	5.065	1.829	80.00	356.171	14.795	179.62	10.652	1.855
0.34	4.986	1.829	84.00	358.054	14.921	179.63	10.575	1.855
0.35	4.906	1.828	88.00	359.912	14.989	179.64	10.498	1.854
0.36	4.826	1.828	92.00	1.762	15.001	179.65	10.421	1.854
0.37	4.746	1.828	96.00	3.623	14.956	179.66	10.343	1.853
0.38	4.666	1.828	100.00	5.512	14.854	179.67	10.266	1.853
0.39	4.586	1.828	104.00	7.447	14.696	179.68	10.189	1.852
0.40	4.506	1.828	108.00	9.448	14.480	179.69	10.111	1.852
0.50	3.706	1.826	112.00	11.531	14.206	179.70	10.034	1.851
0.60	2.904	1.825	116.00	13.715	13.874	179.71	9.956	1.851
0.70	2.102	1.825	120.00	16.015	13.484	179.72	9.878	1.850
0.80	1.299	1.825	124.00	18.446	13.034	179.73	9.801	1.850
0.90	0.498	1.826	128.00	21.023	12.524	179.74	9.723	1.849
1.00	359.697	1.827	132.00	23.753	11.953	179.75	9.645	1.849
1.10	358.897	1.829	136.00	26.638	11.321	179.76	9.567	1.848
1.20	358.100	1.831	140.00	29.674	10.627	179.77	9.489	1.848
1.30	357.305	1.834	144.00	32.839	9.871	179.78	9.411	1.847
1.40	356.513	1.837	148.00	36.089	9.054	179.79	9.333	1.847
1.50	355.725	1.840	152.00	39.348	8.177	179.80	9.256	1.846
1.60	354.941	1.845	156.00	42.477	7.244	179.81	9.177	1.846
1.70	354.161	1.849	160.00	45.235	6.262	179.82	9.099	1.845
1.80	353.386	1.854	164.00	47.180	5.241	179.83	9.021	1.845
1.90	352.617	1.860	164.50	47.180	5.241	179.84	8.943	1.844
2.00	351.853	1.866	165.00	47.180	5.241	179.85	8.865	1.844
2.20	350.345	1.879	165.50	47.180	5.241	179.86	8.786	1.844
2.40	348.865	1.895	166.00	47.180	5.241	179.87	8.708	1.843
2.60	347.416	1.912	166.50	47.180	5.241	179.88	8.630	1.843
2.80	346.000	1.931	167.00	47.180	5.241	179.89	8.551	1.842
3.00	344.619	1.952	167.50	47.180	5.241	179.90	8.473	1.842
3.20	343.274	1.974	168.00	47.180	5.241	179.91	8.394	1.841
3.40	341.969	1.998	170.00	46.418	3.692	179.92	8.316	1.841
3.60	340.703	2.023	171.00	45.463	3.441	179.93	8.237	1.841
3.80	339.477	2.050	172.00	44.123	3.195	179.94	8.158	1.840
4.00	338.292	2.078	173.00	42.312	2.957	179.95	8.080	1.840
4.20	337.149	2.108	174.00	39.925	2.728	179.96	8.001	1.839
4.40	336.046	2.138	174.20	39.368	2.684	179.97	7.922	1.839
4.60	334.985	2.170	174.40	38.782	2.641	179.98	7.844	1.839
4.80	333.965	2.204	174.60	38.166	2.598	179.99	7.765	1.838
5.00	332.985	2.238	174.80	37.519	2.555	180.00	7.686	1.838

$n_0 = 1.4956$, $n_1 = 1.484$, $\lambda = 5461$ Å

SMALL DELTA	DELTA	PSI	SMALL DELTA	DELTA	PSI	SMALL DELTA	DELTA	PSI
0.00	7.686	1.838	5.20	356.900	1.860	175.00	17.299	1.947
0.01	7.665	1.838	5.40	356.502	1.863	175.20	16.953	1.940
0.02	7.644	1.838	5.60	356.107	1.867	175.40	16.603	1.934
0.03	7.624	1.838	5.80	355.714	1.871	175.60	16.249	1.928
0.04	7.603	1.838	6.00	355.323	1.875	175.80	15.892	1.922
0.05	7.582	1.838	7.00	353.416	1.899	176.00	15.531	1.916
0.06	7.562	1.837	8.00	351.592	1.928	176.20	15.166	1.910
0.07	7.541	1.837	9.00	349.860	1.960	176.40	14.798	1.905
0.08	7.520	1.837	10.00	348.228	1.997	176.60	14.426	1.899
0.09	7.499	1.837	12.00	345.282	2.082	176.80	14.051	1.894
0.10	7.479	1.837	12.50	344.614	2.106	177.00	13.673	1.889
0.11	7.458	1.837	13.00	343.973	2.130	177.20	13.292	1.884
0.12	7.437	1.837	13.50	343.359	2.155	177.40	12.908	1.880
0.13	7.416	1.837	14.00	342.772	2.180	177.60	12.521	1.875
0.14	7.396	1.837	14.50	342.212	2.207	177.80	12.130	1.871
0.15	7.375	1.837	15.00	341.679	2.234	178.00	11.738	1.867
0.16	7.354	1.837	15.50	341.172	2.261	178.10	11.540	1.865
0.17	7.333	1.836	16.00	340.690	2.289	178.20	11.342	1.863
0.18	7.313	1.836	20.00	337.698	2.531	178.30	11.144	1.861
0.19	7.292	1.836	24.00	336.026	2.793	178.40	10.944	1.860
0.20	7.271	1.836	28.00	335.375	3.066	178.50	10.744	1.858
0.21	7.250	1.836	32.00	335.495	3.342	178.60	10.544	1.856
0.22	7.230	1.836	36.00	336.187	3.614	178.70	10.343	1.855
0.23	7.209	1.836	40.00	337.301	3.878	178.80	10.141	1.853
0.24	7.188	1.836	44.00	338.725	4.131	178.90	9.939	1.852
0.25	7.167	1.836	48.00	340.377	4.370	179.00	9.737	1.850
0.26	7.146	1.836	52.00	342.195	4.593	179.10	9.534	1.849
0.27	7.126	1.836	56.00	344.133	4.799	179.20	9.330	1.847
0.28	7.105	1.836	60.00	346.157	4.985	179.30	9.126	1.846
0.29	7.084	1.835	64.00	348.242	5.152	179.40	8.921	1.845
0.30	7.063	1.835	68.00	350.371	5.298	179.50	8.717	1.843
0.31	7.043	1.835	72.00	352.529	5.422	179.60	8.511	1.842
0.32	7.022	1.835	76.00	354.708	5.525	179.61	8.491	1.842
0.33	7.001	1.835	80.00	356.902	5.605	179.62	8.470	1.842
0.34	6.980	1.835	84.00	359.106	5.662	179.63	8.449	1.842
0.35	6.959	1.835	88.00	1.318	5.696	179.64	8.429	1.842
0.36	6.939	1.835	92.00	3.535	5.708	179.65	8.408	1.842
0.37	6.918	1.835	96.00	5.757	5.695	179.66	8.388	1.842
0.38	6.897	1.835	100.00	7.982	5.660	179.67	8.367	1.841
0.39	6.876	1.835	104.00	10.208	5.602	179.68	8.347	1.841
0.40	6.855	1.835	108.00	12.432	5.521	179.69	8.326	1.841
0.50	6.647	1.834	112.00	14.648	5.417	179.70	8.305	1.841
0.60	6.438	1.833	116.00	16.850	5.291	179.71	8.285	1.841
0.70	6.229	1.833	120.00	19.029	5.144	179.72	8.264	1.841
0.80	6.020	1.832	124.00	21.169	4.975	179.73	8.244	1.841
0.90	5.811	1.832	128.00	23.250	4.787	179.74	8.223	1.841
1.00	5.602	1.831	132.00	25.247	4.580	179.75	8.202	1.841
1.10	5.392	1.831	136.00	27.122	4.355	179.76	8.182	1.840
1.20	5.183	1.830	140.00	28.828	4.113	179.77	8.161	1.840
1.30	4.973	1.830	144.00	30.299	3.859	179.78	8.140	1.840
1.40	4.763	1.830	148.00	31.448	3.593	179.79	8.120	1.840
1.50	4.553	1.830	152.00	32.158	3.319	179.80	8.099	1.840
1.60	4.343	1.830	156.00	32.272	3.043	179.81	8.079	1.840
1.70	4.133	1.830	160.00	31.586	2.769	179.82	8.058	1.840
1.80	3.923	1.829	164.00	29.841	2.507	179.83	8.037	1.840
1.90	3.713	1.830	164.50	29.841	2.507	179.84	8.017	1.840
2.00	3.503	1.830	165.00	29.841	2.507	179.85	7.996	1.839
2.20	3.083	1.830	165.50	29.841	2.507	179.86	7.975	1.839
2.40	2.663	1.830	166.00	29.841	2.507	179.87	7.955	1.839
2.60	2.244	1.831	166.50	29.841	2.507	179.88	7.934	1.839
2.80	1.825	1.832	167.00	29.841	2.507	179.89	7.913	1.839
3.00	1.408	1.833	167.50	29.841	2.507	179.90	7.893	1.839
3.20	0.991	1.835	168.00	29.841	2.507	179.91	7.872	1.839
3.40	0.575	1.836	170.00	24.581	2.161	179.92	7.851	1.839
3.60	0.160	1.838	171.00	23.342	2.111	179.93	7.831	1.839
3.80	359.746	1.840	172.00	21.993	2.065	179.94	7.810	1.839
4.00	359.334	1.842	173.00	20.535	2.022	179.95	7.789	1.838
4.20	358.924	1.845	174.00	18.969	1.982	179.96	7.769	1.838
4.40	358.515	1.847	174.20	18.643	1.975	179.97	7.748	1.838
4.60	358.108	1.850	174.40	18.313	1.968	179.98	7.727	1.838
4.80	357.704	1.853	174.60	17.979	1.961	179.99	7.707	1.838
5.00	357.301	1.856	174.80	17.641	1.954	180.00	7.686	1.838

$n_0 = 1.4992$, $n_1 = 1.460$, $\lambda = 5461$ Å

SMALL DELTA	DELTA	PSI	SMALL DELTA	DELTA	PSI	SMALL DELTA	DELTA	PSI
0.00	7.335	1.928	5.20	329.780	2.472	175.00	38.133	2.720
0.01	7.250	1.927	5.40	328.891	2.516	175.20	37.421	2.672
0.02	7.164	1.927	5.60	328.045	2.560	175.40	36.671	2.625
0.03	7.078	1.927	5.80	327.240	2.606	175.60	35.882	2.579
0.04	6.992	1.926	6.00	326.474	2.653	175.80	35.053	2.534
0.05	6.907	1.926	7.00	323.189	2.897	176.00	34.181	2.490
0.06	6.821	1.926	8.00	320.694	3.158	176.20	33.267	2.447
0.07	6.735	1.925	9.00	318.838	3.430	176.40	32.309	2.405
0.08	6.649	1.925	10.00	317.498	3.711	176.60	31.306	2.364
0.09	6.563	1.924	12.00	315.976	4.288	176.80	30.256	2.325
0.10	6.477	1.924	12.50	315.783	4.434	177.00	29.159	2.287
0.11	6.391	1.924	13.00	315.651	4.580	177.20	28.015	2.250
0.12	6.305	1.924	13.50	315.573	4.727	177.40	26.823	2.215
0.13	6.218	1.923	14.00	315.544	4.874	177.60	25.582	2.181
0.14	6.132	1.923	14.50	315.560	5.021	177.80	24.294	2.149
0.15	6.046	1.923	15.00	315.616	5.168	178.00	22.957	2.119
0.16	5.960	1.922	15.50	315.708	5.315	178.10	22.272	2.105
0.17	5.873	1.922	16.00	315.834	5.462	178.20	21.574	2.091
0.18	5.787	1.922	20.00	317.709	6.619	178.30	20.865	2.077
0.19	5.701	1.921	24.00	320.501	7.733	178.40	20.145	2.064
0.20	5.614	1.921	28.00	323.684	8.789	178.50	19.413	2.051
0.21	5.528	1.921	32.00	326.983	9.780	178.60	18.671	2.039
0.22	5.442	1.921	36.00	330.248	10.703	178.70	17.918	2.028
0.23	5.355	1.920	40.00	333.398	11.556	178.80	17.155	2.017
0.24	5.269	1.920	44.00	336.392	12.339	178.90	16.382	2.006
0.25	5.182	1.920	48.00	339.211	13.052	179.00	15.599	1.996
0.26	5.096	1.920	52.00	341.852	13.697	179.10	14.807	1.987
0.27	5.009	1.919	56.00	344.323	14.275	179.20	14.006	1.978
0.28	4.923	1.919	60.00	346.636	14.786	179.30	13.197	1.970
0.29	4.836	1.919	64.00	348.807	15.233	179.40	12.379	1.962
0.30	4.749	1.919	68.00	350.852	15.615	179.50	11.555	1.955
0.31	4.663	1.919	72.00	352.793	15.934	179.60	10.723	1.948
0.32	4.576	1.918	76.00	354.647	16.191	179.61	10.639	1.948
0.33	4.489	1.918	80.00	356.434	16.386	179.62	10.555	1.947
0.34	4.403	1.918	84.00	358.174	16.519	179.63	10.472	1.946
0.35	4.316	1.918	88.00	359.886	16.592	179.64	10.388	1.946
0.36	4.229	1.918	92.00	1.590	16.603	179.65	10.304	1.945
0.37	4.142	1.917	96.00	3.304	16.554	179.66	10.220	1.945
0.38	4.056	1.917	100.00	5.049	16.443	179.67	10.136	1.944
0.39	3.969	1.917	104.00	6.844	16.271	179.68	10.052	1.943
0.40	3.882	1.917	108.00	8.709	16.037	179.69	9.968	1.943
0.50	3.013	1.916	112.00	10.662	15.741	179.70	9.884	1.942
0.60	2.143	1.915	116.00	12.725	15.382	179.71	9.800	1.942
0.70	1.273	1.915	120.00	14.915	14.959	179.72	9.716	1.941
0.80	0.403	1.916	124.00	17.253	14.471	179.73	9.631	1.941
0.90	359.534	1.917	128.00	19.753	13.916	179.74	9.547	1.940
1.00	358.668	1.919	132.00	22.430	13.294	179.75	9.463	1.939
1.10	357.803	1.922	136.00	25.293	12.604	179.76	9.378	1.939
1.20	356.942	1.925	140.00	28.340	11.844	179.77	9.294	1.938
1.30	356.084	1.929	144.00	31.559	11.013	179.78	9.209	1.938
1.40	355.230	1.933	148.00	34.916	10.111	179.79	9.124	1.937
1.50	354.382	1.938	152.00	38.340	9.139	179.80	9.040	1.937
1.60	353.539	1.943	156.00	41.705	8.099	179.81	8.955	1.936
1.70	352.702	1.950	160.00	44.781	6.998	179.82	8.870	1.936
1.80	351.872	1.956	164.00	47.139	5.847	179.83	8.785	1.935
1.90	351.048	1.964	164.50	47.139	5.847	179.84	8.700	1.935
2.00	350.233	1.972	165.00	47.139	5.847	179.85	8.615	1.934
2.20	348.627	1.989	165.50	47.139	5.847	179.86	8.530	1.934
2.40	347.056	2.009	166.00	47.139	5.847	179.87	8.445	1.933
2.60	345.525	2.030	166.50	47.139	5.847	179.88	8.360	1.933
2.80	344.035	2.054	167.00	47.139	5.847	179.89	8.275	1.932
3.00	342.588	2.080	167.50	47.139	5.847	179.90	8.190	1.932
3.20	341.187	2.108	168.00	47.139	5.847	179.91	8.105	1.932
3.40	339.833	2.137	170.00	47.174	4.083	179.92	8.019	1.931
3.60	338.526	2.168	171.00	46.362	3.794	179.93	7.934	1.931
3.80	337.266	2.201	172.00	45.159	3.511	179.94	7.849	1.930
4.00	336.055	2.236	173.00	43.470	3.235	179.95	7.763	1.930
4.20	334.893	2.272	174.00	41.175	2.970	179.96	7.678	1.929
4.40	333.777	2.309	174.20	40.632	2.919	179.97	7.592	1.929
4.60	332.709	2.348	174.40	40.057	2.868	179.98	7.507	1.929
4.80	331.688	2.388	174.60	39.450	2.818	179.99	7.421	1.928
5.00	330.712	2.430	174.80	38.809	2.769	180.00	7.335	1.928

$n_0 = 1.4992$, $n_1 = 1.484$, $\lambda = 5461\,\text{Å}$

SMALL DELTA	DELTA	PSI	SMALL DELTA	DELTA	PSI	SMALL DELTA	DELTA	PSI
0.00	7.335	1.928	5.20	353.659	1.974	175.00	19.420	2.083
0.01	7.309	1.928	5.40	353.166	1.980	175.20	18.998	2.073
0.02	7.282	1.928	5.60	352.679	1.986	175.40	18.569	2.064
0.03	7.256	1.927	5.80	352.196	1.993	175.60	18.135	2.055
0.04	7.229	1.927	6.00	351.718	2.000	175.80	17.694	2.046
0.05	7.203	1.927	7.00	349.405	2.038	176.00	17.248	2.038
0.06	7.176	1.927	8.00	347.234	2.083	176.20	16.796	2.029
0.07	7.150	1.927	9.00	345.214	2.135	176.40	16.339	2.022
0.08	7.123	1.927	10.00	343.353	2.191	176.60	15.876	2.014
0.09	7.097	1.927	12.00	340.109	2.320	176.80	15.408	2.006
0.10	7.070	1.927	12.50	339.397	2.355	177.00	14.935	1.999
0.11	7.044	1.926	13.00	338.723	2.391	177.20	14.457	1.992
0.12	7.017	1.926	13.50	338.086	2.427	177.40	13.974	1.986
0.13	6.991	1.926	14.00	337.486	2.465	177.60	13.486	1.979
0.14	6.964	1.926	14.50	336.921	2.503	177.80	12.994	1.974
0.15	6.938	1.926	15.00	336.391	2.542	178.00	12.497	1.968
0.16	6.911	1.926	15.50	335.895	2.582	178.10	12.247	1.965
0.17	6.884	1.926	16.00	335.432	2.623	178.20	11.996	1.962
0.18	6.858	1.926	20.00	332.770	2.965	178.30	11.744	1.960
0.19	6.831	1.926	24.00	331.608	3.326	178.40	11.491	1.957
0.20	6.805	1.926	28.00	331.515	3.695	178.50	11.238	1.955
0.21	6.778	1.925	32.00	332.173	4.061	178.60	10.983	1.953
0.22	6.751	1.925	36.00	333.355	4.418	178.70	10.727	1.950
0.23	6.725	1.925	40.00	334.902	4.761	178.80	10.471	1.948
0.24	6.698	1.925	44.00	336.700	5.086	178.90	10.213	1.946
0.25	6.672	1.925	48.00	338.670	5.391	179.00	9.955	1.944
0.26	6.645	1.925	52.00	340.754	5.674	179.10	9.696	1.942
0.27	6.618	1.925	56.00	342.912	5.934	179.20	9.437	1.940
0.28	6.592	1.925	60.00	345.116	6.168	179.30	9.176	1.938
0.29	6.565	1.925	64.00	347.346	6.376	179.40	8.915	1.936
0.30	6.539	1.924	68.00	349.588	6.558	179.50	8.653	1.935
0.31	6.512	1.924	72.00	351.836	6.712	179.60	8.391	1.933
0.32	6.485	1.924	76.00	354.084	6.838	179.61	8.365	1.933
0.33	6.459	1.924	80.00	356.331	6.936	179.62	8.338	1.933
0.34	6.432	1.924	84.00	358.577	7.005	179.63	8.312	1.933
0.35	6.405	1.924	88.00	0.823	7.046	179.64	8.286	1.933
0.36	6.379	1.924	92.00	3.071	7.058	179.65	8.259	1.933
0.37	6.352	1.924	96.00	5.325	7.040	179.66	8.233	1.932
0.38	6.326	1.924	100.00	7.586	6.994	179.67	8.207	1.932
0.39	6.299	1.924	104.00	9.856	6.919	179.68	8.180	1.932
0.40	6.272	1.924	108.00	12.137	6.816	179.69	8.154	1.932
0.50	6.005	1.923	112.00	14.428	6.684	179.70	8.128	1.932
0.60	5.738	1.922	116.00	16.726	6.524	179.71	8.102	1.932
0.70	5.471	1.921	120.00	19.025	6.336	179.72	8.075	1.931
0.80	5.203	1.921	124.00	21.315	6.122	179.73	8.049	1.931
0.90	4.935	1.920	128.00	23.581	5.882	179.74	8.022	1.931
1.00	4.667	1.920	132.00	25.799	5.616	179.75	7.996	1.931
1.10	4.399	1.919	136.00	27.939	5.327	179.76	7.970	1.931
1.20	4.131	1.919	140.00	29.954	5.016	179.77	7.943	1.931
1.30	3.862	1.919	144.00	31.782	4.685	179.78	7.917	1.931
1.40	3.594	1.919	148.00	33.328	4.337	179.79	7.891	1.930
1.50	3.325	1.919	152.00	34.472	3.976	179.80	7.864	1.930
1.60	3.057	1.919	156.00	35.036	3.607	179.81	7.838	1.930
1.70	2.788	1.919	160.00	34.770	3.238	179.82	7.811	1.930
1.80	2.520	1.919	164.00	33.326	2.878	179.83	7.785	1.930
1.90	2.251	1.919	164.50	33.326	2.878	179.84	7.759	1.930
2.00	1.983	1.920	165.00	33.326	2.878	179.85	7.732	1.930
2.20	1.447	1.921	165.50	33.326	2.878	179.86	7.706	1.930
2.40	0.912	1.922	166.00	33.326	2.878	179.87	7.679	1.929
2.60	0.378	1.924	166.50	33.326	2.878	179.88	7.653	1.929
2.80	359.846	1.926	167.00	33.326	2.878	179.89	7.627	1.929
3.00	359.315	1.928	167.50	33.326	2.878	179.90	7.600	1.929
3.20	358.787	1.931	168.00	33.326	2.878	179.91	7.574	1.929
3.40	358.260	1.933	170.00	27.922	2.391	179.92	7.547	1.929
3.60	357.736	1.937	171.00	26.539	2.320	179.93	7.521	1.929
3.80	357.215	1.940	172.00	25.003	2.253	179.94	7.494	1.929
4.00	356.696	1.944	173.00	23.300	2.191	179.95	7.468	1.928
4.20	356.181	1.948	174.00	21.440	2.134	179.96	7.441	1.928
4.40	355.669	1.953	174.20	21.048	2.123	179.97	7.415	1.928
4.60	355.160	1.958	174.40	20.651	2.113	179.98	7.388	1.928
4.80	354.656	1.963	174.60	20.247	2.103	179.99	7.362	1.928
5.00	354.155	1.968	174.80	19.836	2.093	180.00	7.335	1.928